Space Climate 7, Orford, July 11

Solar Wind influences on the Ionosphere-Earth Current Density and its influence on Clouds

Brian A. Tinsley
University of Texas at Dallas
tinsley@UTDallas.edu
http://www.utdallas.edu/physics/tinsley-brian

OUTLINE

The Space-Weather – Atmospheric Electricity – Surface Weather Connection

Direct effects of ionosphere-earth current density (Jz) on polar stratus-type tropospheric clouds

- (a) Response of clouds to Jz changes due to day-to-day variations of Ez at Vostok, with and without the solar wind input
- (b) Response of polar ionospheric potential to IMF By
- (c) Response of clouds to IMF By
- (d) Response of clouds to magnetic Ap (electrojet) variations
- (e) Response of clouds to By in superposed epoch analysis
- (f) Responses of clouds to two and four sector solar wind regimes

Parameterizing the ionospheric potential: Bz and Vsw

- (a) Parameterizing the potential at the pole
- (b) Parameterizing the integrated whole polar cap potential
- (c) Decadal and semi-annual variations of ionospheric potential

Proposed mechanism for stratus-type clouds

Indirect effects at solar wind sector boundaries; solar wind speed, relativistic electrons and volcanic aerosols

Decadal effects on clouds and the NAO and volcanic aerosols (also in M 10 and JA 05).

Conclusions and wider implications

THE ELECTRICAL CONNECTION

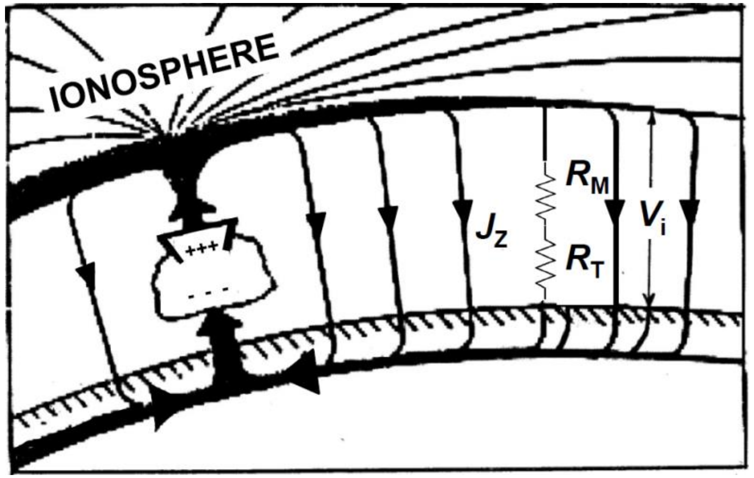

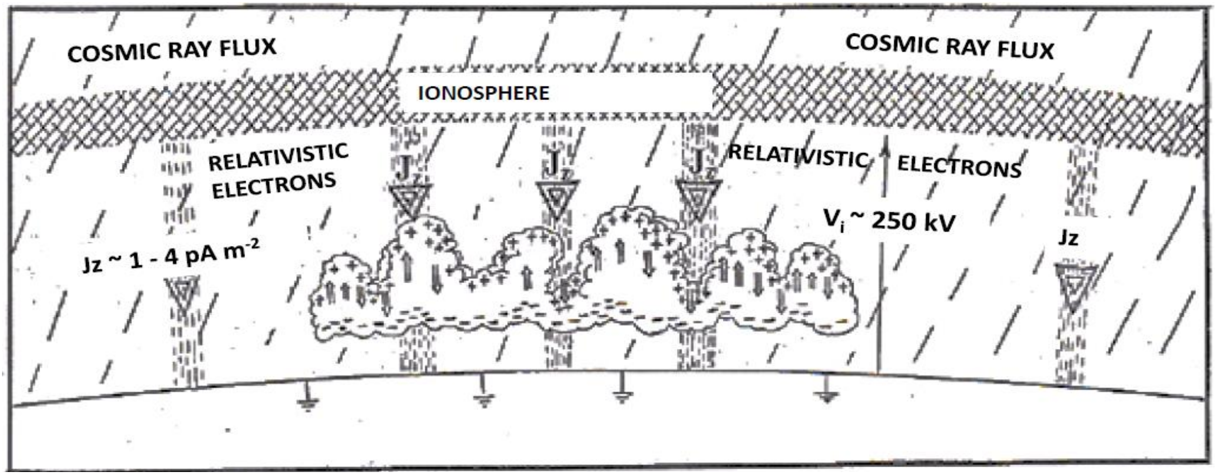

Cosmic rays and other space particle fluxes weakly ionize the atmosphere. Each of about 1000 highly electrified storms around the globe sends about 1 Ampere to the Ionosphere, and it charges to V_{i}~ 250 kV, varying diurnally and from day-to-day.

The local downward current density, J_z, (1-4 pA m^{-2}), is given by Ohm's Law in three dimensions: $J_z = V_i/(R_M + R_T)$ where R_M and R_T are the column resistances (Ω-m^2) of the middle atmosphere and troposphere respectively. Any change in V_i, R_M, or R_T affects J_z. **Changes in J_z have been observed with six different inputs, and short-term changes in clouds and/atmospheric dynamics correlate with each**:

V_i varies with solar wind electric inputs in the Arctic and Antarctic i.e., with **IMF *By*** and with ***Ap*.**

R_M and R_T vary with **cosmic ray flux**,

R_M varies with **relativistic electron flux**, the **solar proton flux**, and **volcanic activity**.

The variations of V_i with globally integrated thunderstorm activity serve as a control.

D.R. Kniveton et al. / Journal of Atmospheric and Solar-Terrestrial Physics 70 (2008) 1633–1642

CHANGES IN CLOUD COVER OVER THE ANTARCTIC PLATEAU

The correlations are with measured E_z at Vostok, 1998-2001.

Key day is maximum or minimum of E_z.

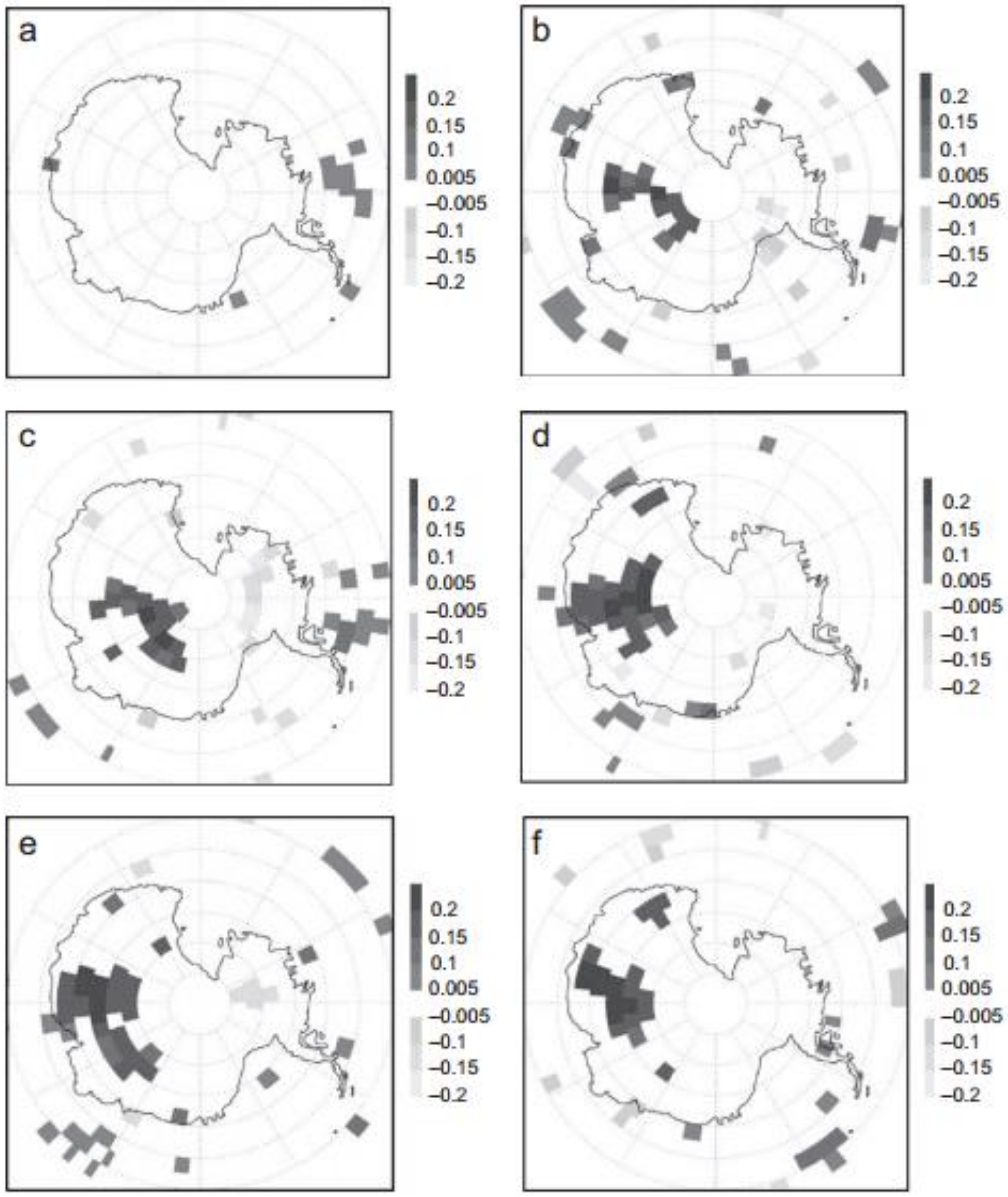

Baseline is 3-5 days before key day.

(a) 3 days before key day.
(b) 2 days before key day
(c) 1 day before key day
(d) Key day
(e) 1 day after hey day
(f) 2 days after key day

From Kniveton et al., 2008.

REGIONAL PRESSURE RESPONSES TO GLOBAL IONOSPHERIC POTENTIAL CHANGES.

From measured Ez at Vostok with solar wind input subtracted.
(Burns Effect)

Zhou et al. 2018

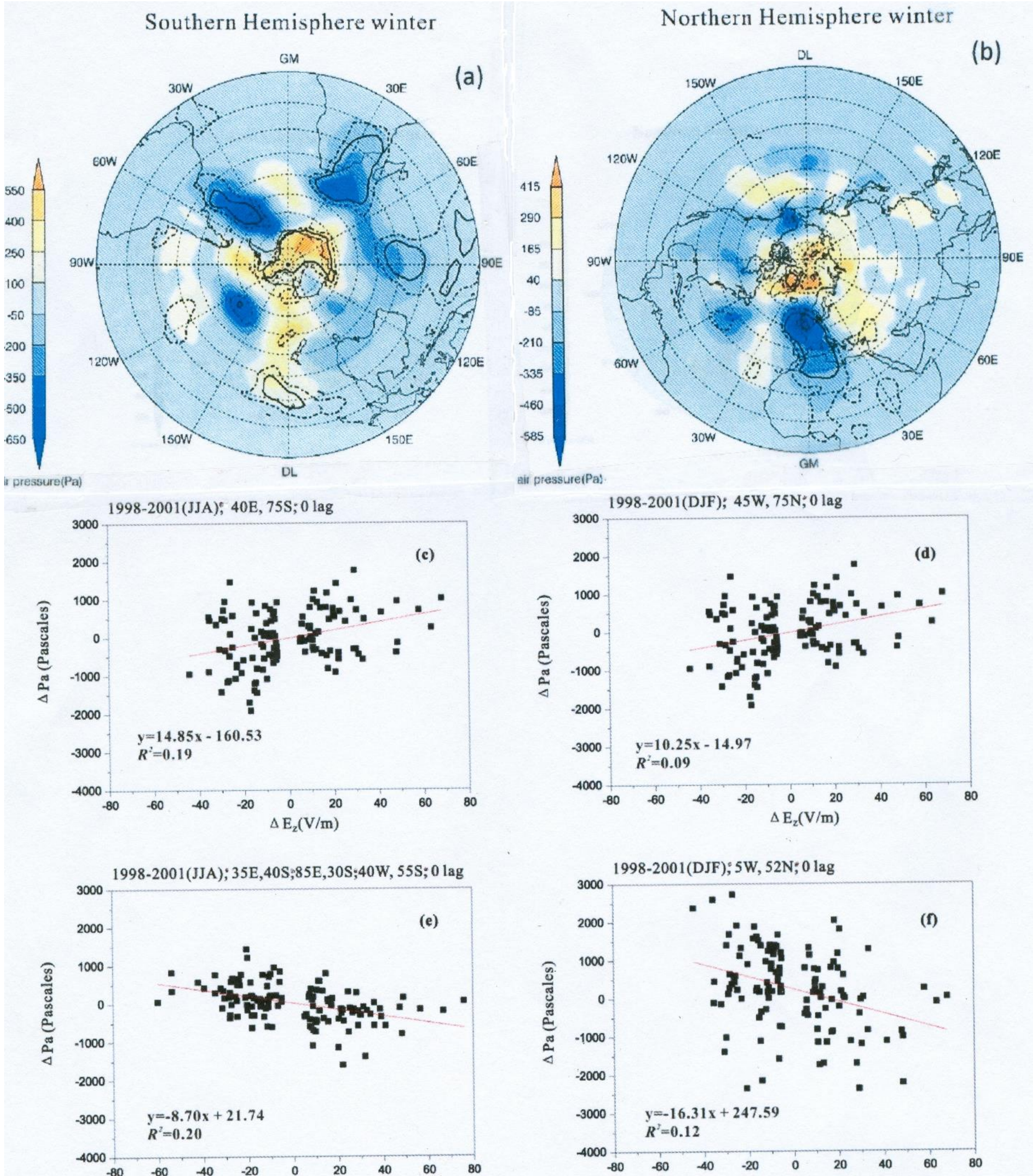

(a) Southern Hemisphere Winter

(b) Northern Hemisphere Winter

(c) Correlation of daily surface pressure and E_z at 75°S
(d) Correlation of daily surface pressure and E_z at 75°N

(e) Correlation of daily surface pressure and E_z for three Sub-Antarctic Locations Averaged
(f) Correlation of daily surface pressure and E_z at 52°N, 5°W.

SOLAR WIND GENERATES MAGNETOSPHERIC ELECTRIC CURRENTS AND SUPERIMPOSES POTENTIALS ON THE POLAR IONOSPHERES

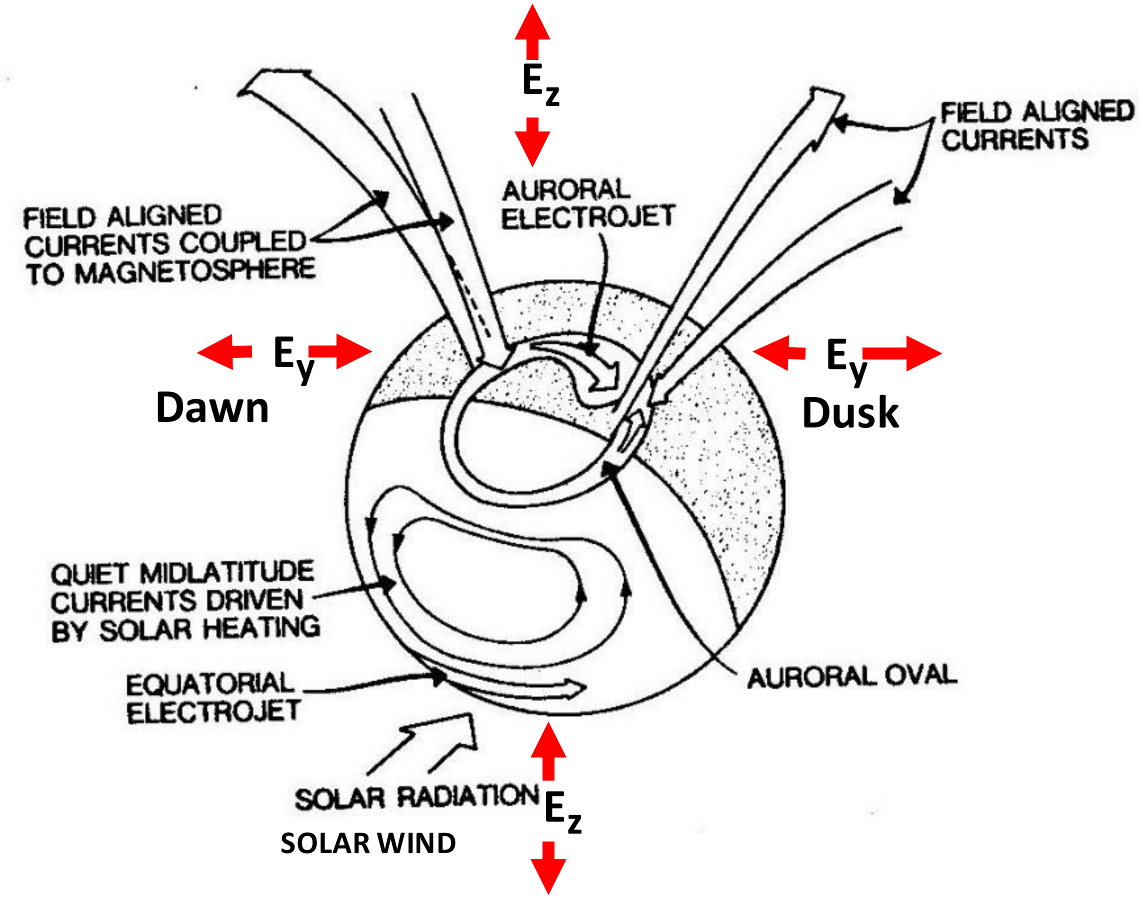

There is a dawn-dusk (east-west) added potential difference, $\mathbf{E_y}$ due to $\mathbf{V_x} \times \mathbf{B_z}$.
There is a north-south (pole to pole) added potential difference, centered on the magnetic poles, $\mathbf{E_z}$ due to $\mathbf{V_x} \times \mathbf{B_y}$. These affect Jz, as do the intensified auroral electrojet currents during magnetic storms.

From Richmond (1986)

THE POTENTIAL PATTERN IS FIXED RELATIVE TO THE LINE TO THE SUN WHILE THE EARTH ROTATES UNDER IT.

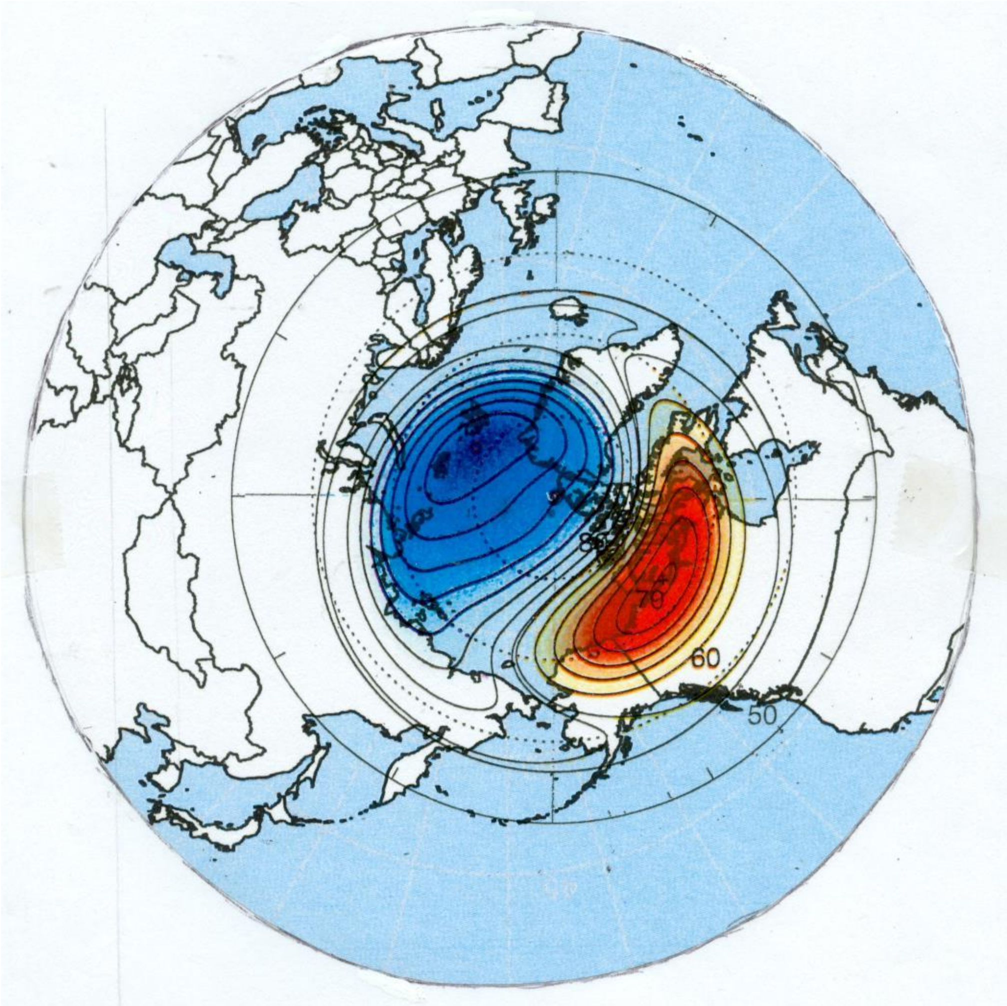

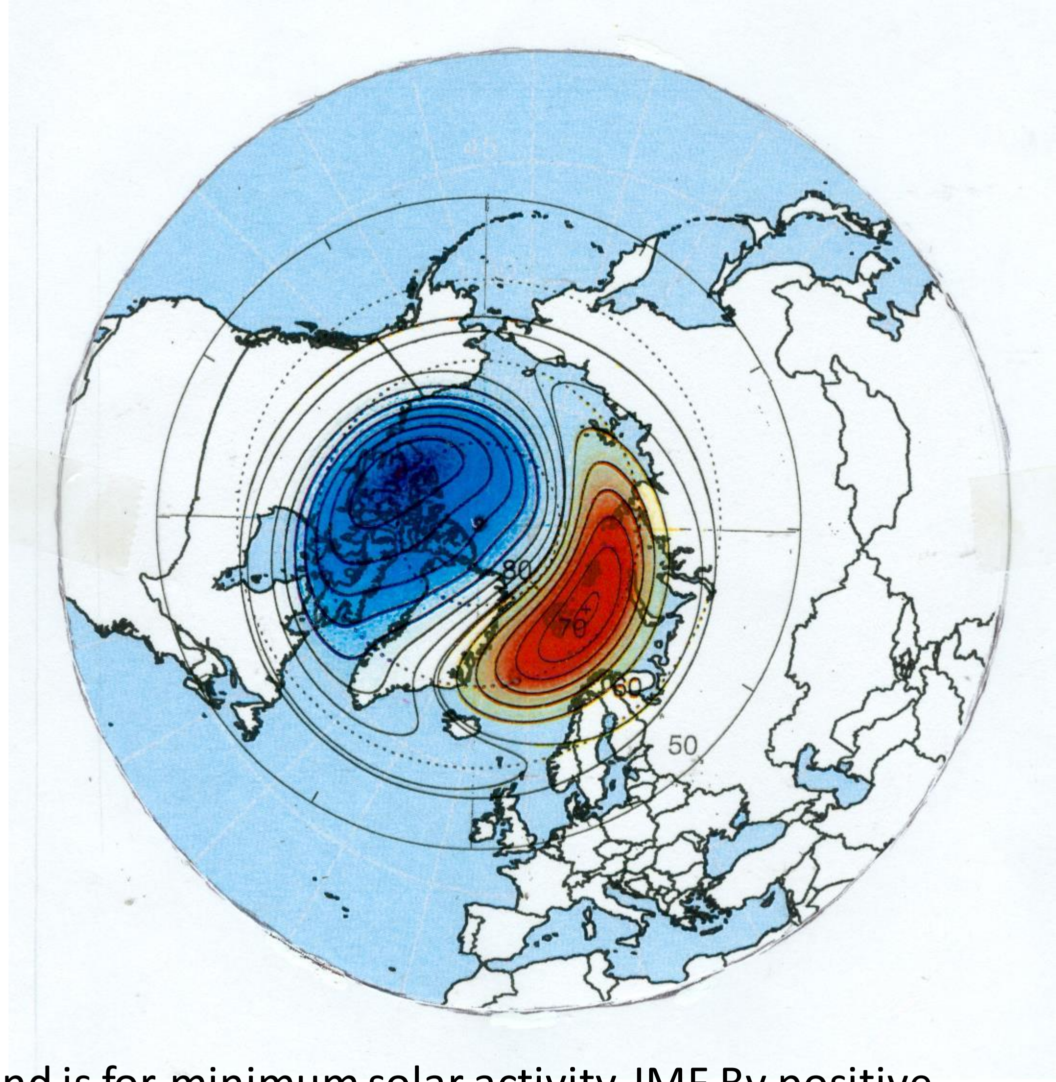

This potential distribution is from Weimer (1996), and is for minimum solar activity, IMF By positive. It expands out beyond outer circle during magnetic storms.

POTENTIAL DISTRIBUTIONS IN THE ARCTIC TO 60° GM LAT.: CHANGING DISTRIBUTIONS FOR IMF B_Y AND B_Z CHANGES, FROM SATELLITE MEASUREMENTS

IMF By Positive adds negative potential, centered on N magnetic pole.

In the Antarctic it adds positive potential

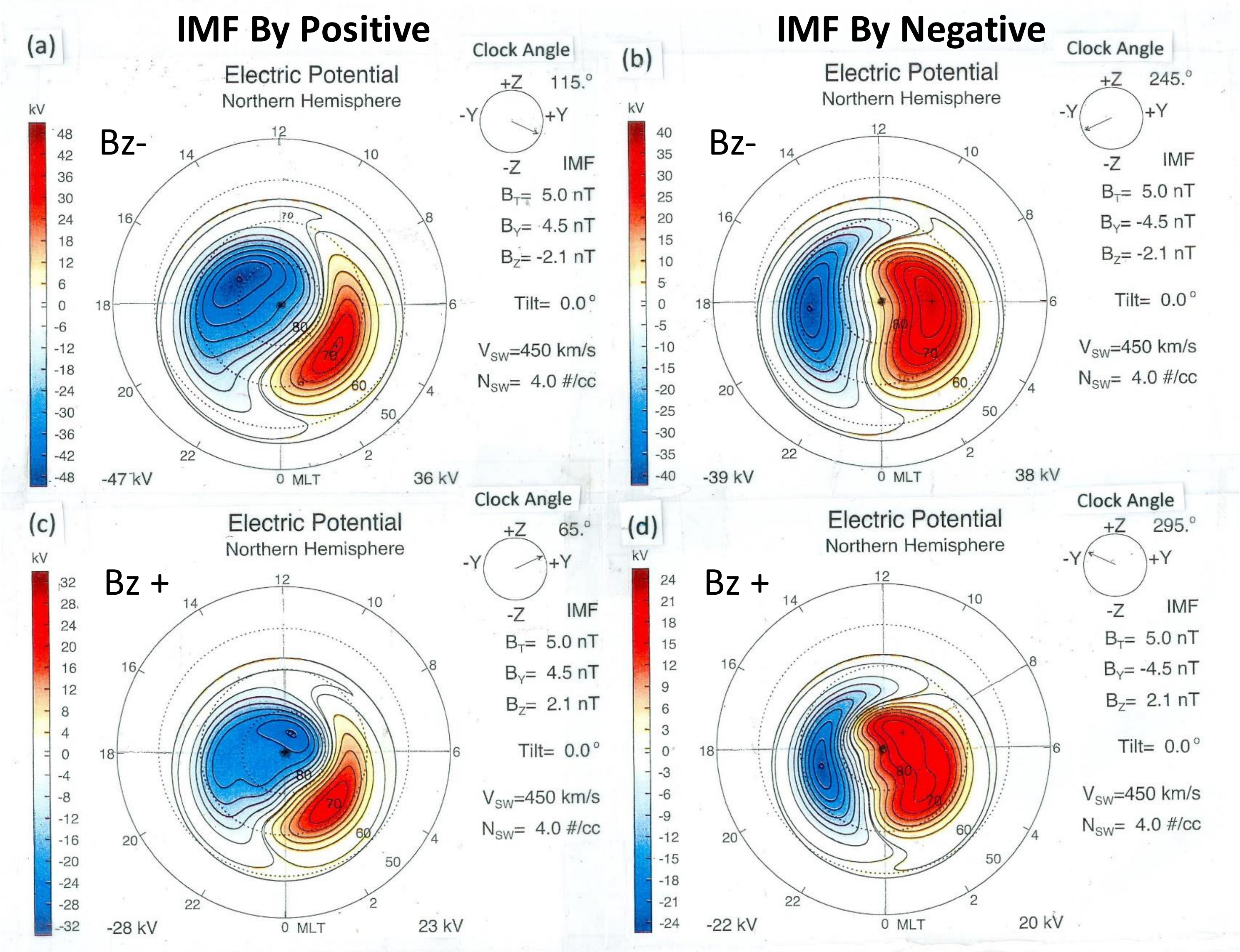

IMF By Negative adds positive potential, centered on N magnetic pole.

In the Antarctic it adds negative potential

From Weimer, 1996

IONOSPHERIC POTENTIAL CHANGES WITH IMF B_Y CHANGE.

From – ve to +ve, relative to a constant dawn-dusk potential pattern. Antarctic (left) and Arctic (right)

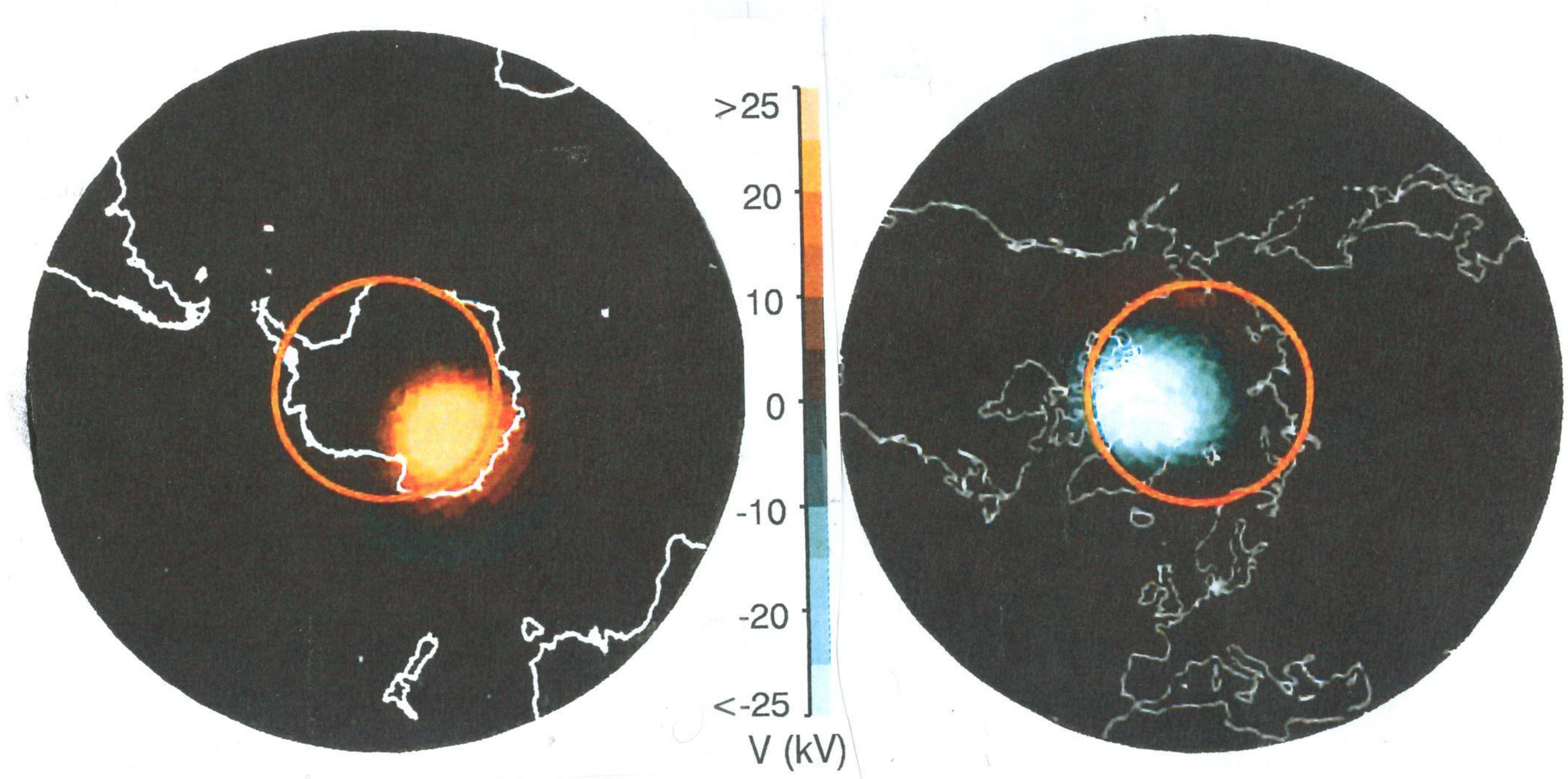

Opposite dependence of polarity of ionospheric potential change in Arctic vs Antarctic
(-ve blue, +ve orange). Derived from Superdarn radar data and the Weimer model.
Potential change in kV.

Lam, Chisham and Freeman, ERL 8, 045001, 2013

RESPONSE OF CLOUD COVER & SURFACE TEMPERATURE TO IMF By INPUT, 2004-2015

Correlations at Alert, Canada, 87 degrees North magnetic latitude.

The change in cloud infrared opacity is measured by looking up at the downwelling longwave infrared irradiance.

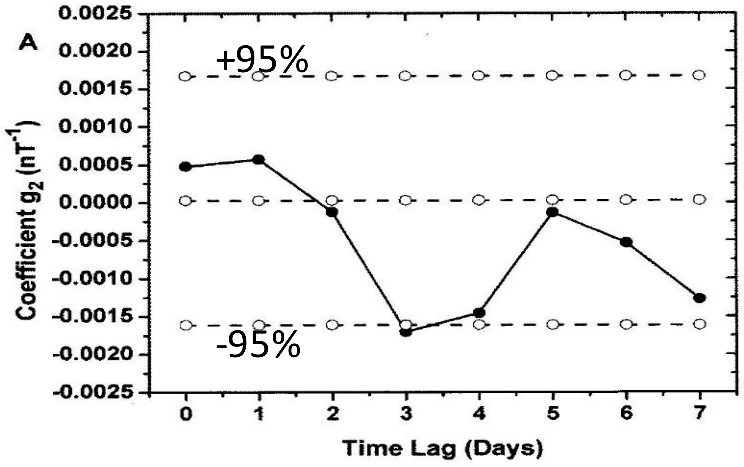

The horizontal axes are the time lag between the IMF *By* time series and the measured cloud opacity in the longwave infrared. (Ionospheric potential and Jz decrease with positive By excursions near the northern magnetic pole).

The surface temperature lags the cloud opacity by one day.

The change in surface temperature is measured by the longwave infrared irradiance looking down (to the surface)

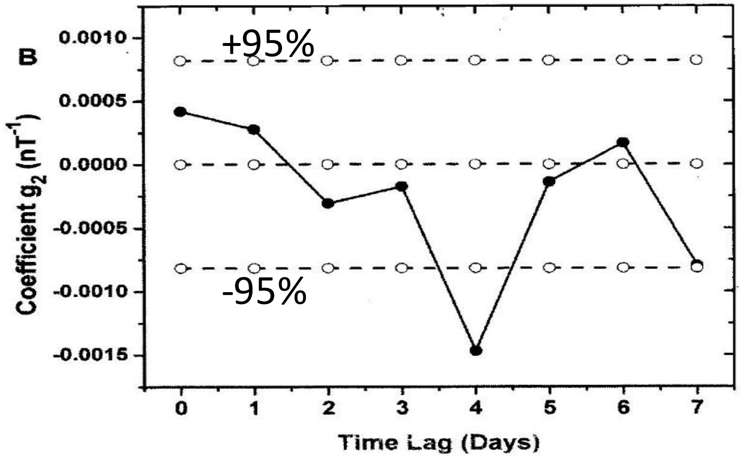

The response amounts to a surface temperature decrease of 0.3C

Frederick and Tinsley, JASTP 2019

SUPERPOSED EPOCH VARIATIONS FOR ALERT LW_IR 2004-2009

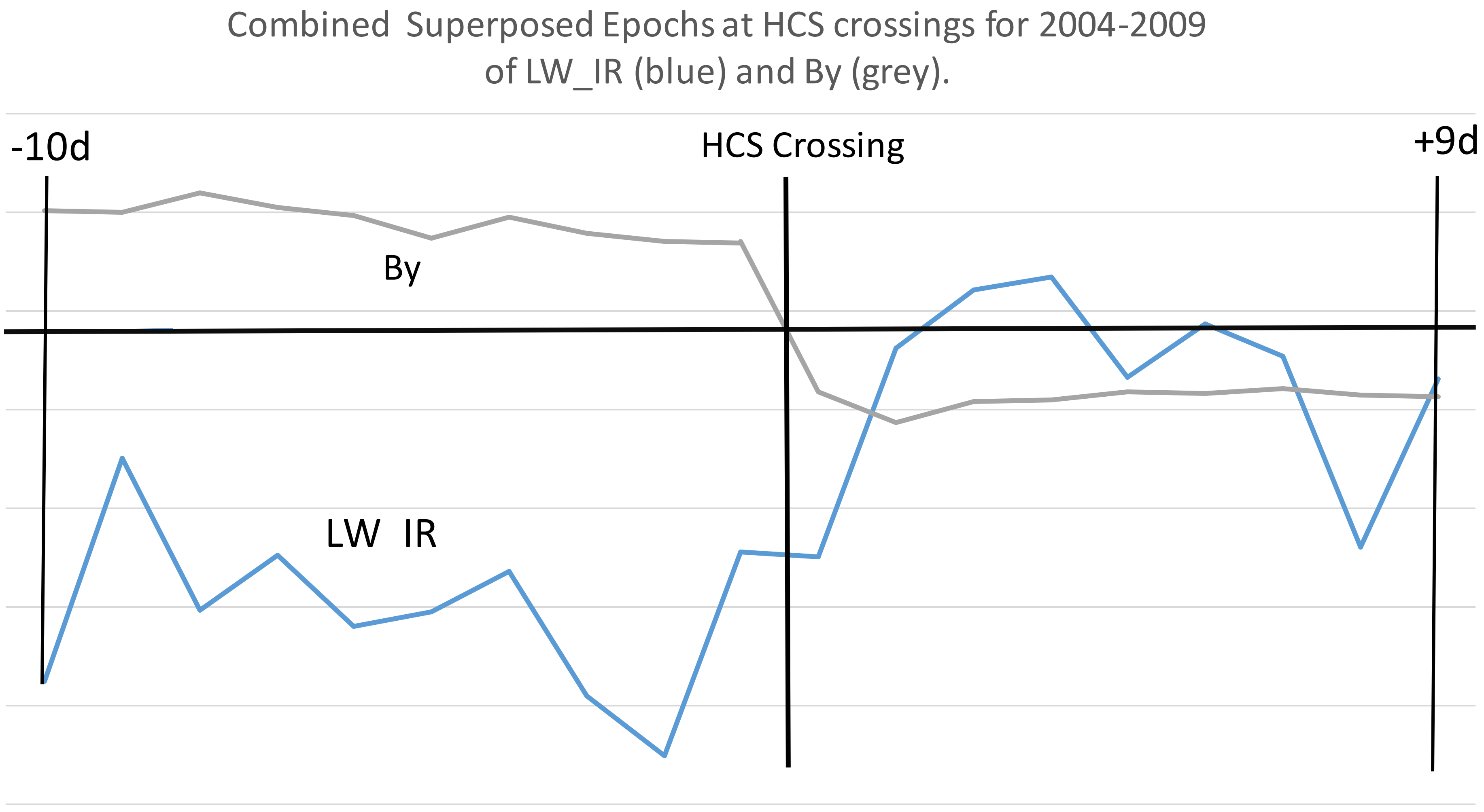

CORRELATION COEFFICIENTS RELATING LONGWAVE DOWNWELLING LONGWAVE INFRARED RADIANCE AT SOUTH POLE

The South Geographic Pole is about 15 degrees from the South Magnetic Pole, and near the Southern auroral electrojets. These correlations are with A_p for time lags -5 to 14 days.

The upper panel is for South Pole daylight with 95% confidence limits for the response on days 1 and 2.

The lower panel is for South Pole darkness, with 95% confidence limits on the responses on days 3 and 4.

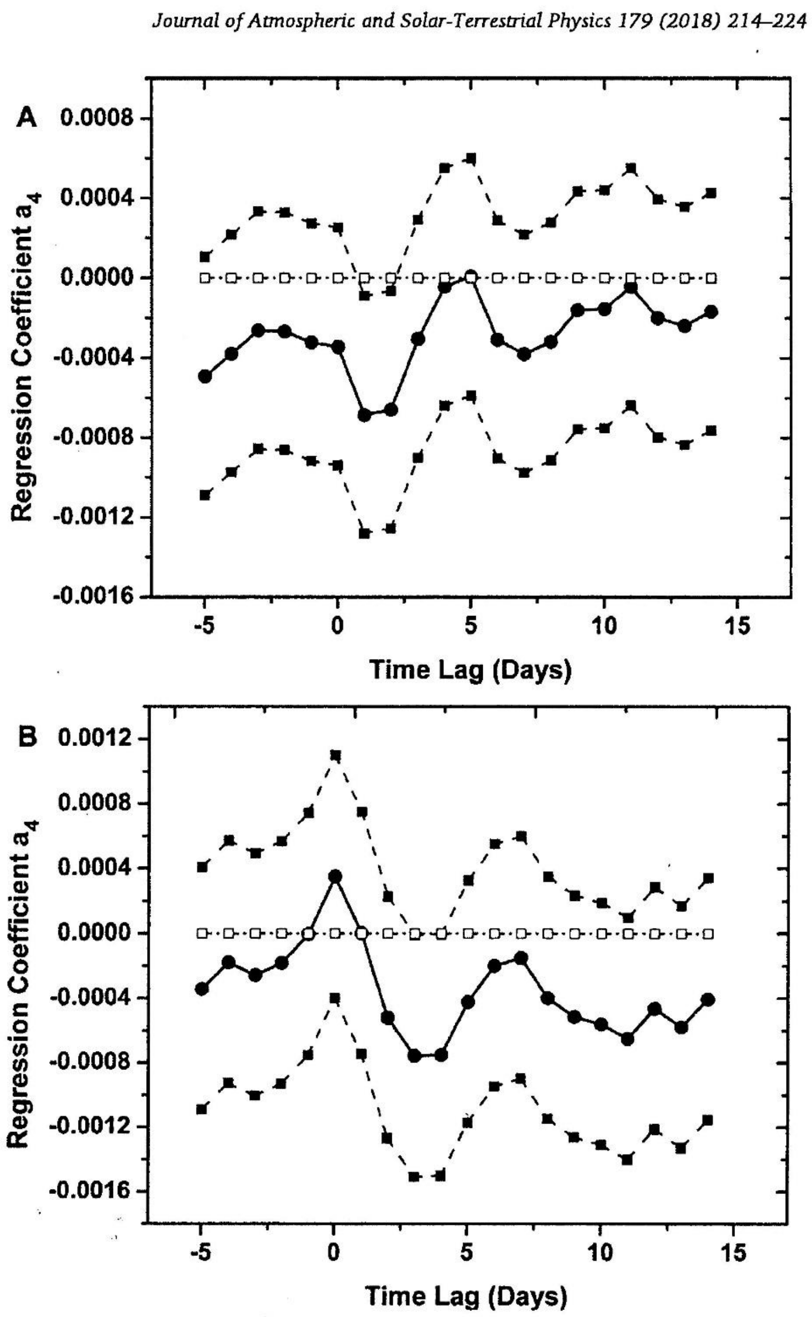

The solid lines denote the best-estimate. The upper and lower dashed curves define the 95% confidence limits.

The lines with open squares are for zero correlation coefficient.

Frederick and Tinsley, JASTP 2018

PARAMETERIZING THE SOLAR WIND IONOSPHERIC POTENTIAL AT THE NORTH MAGNETIC POLE

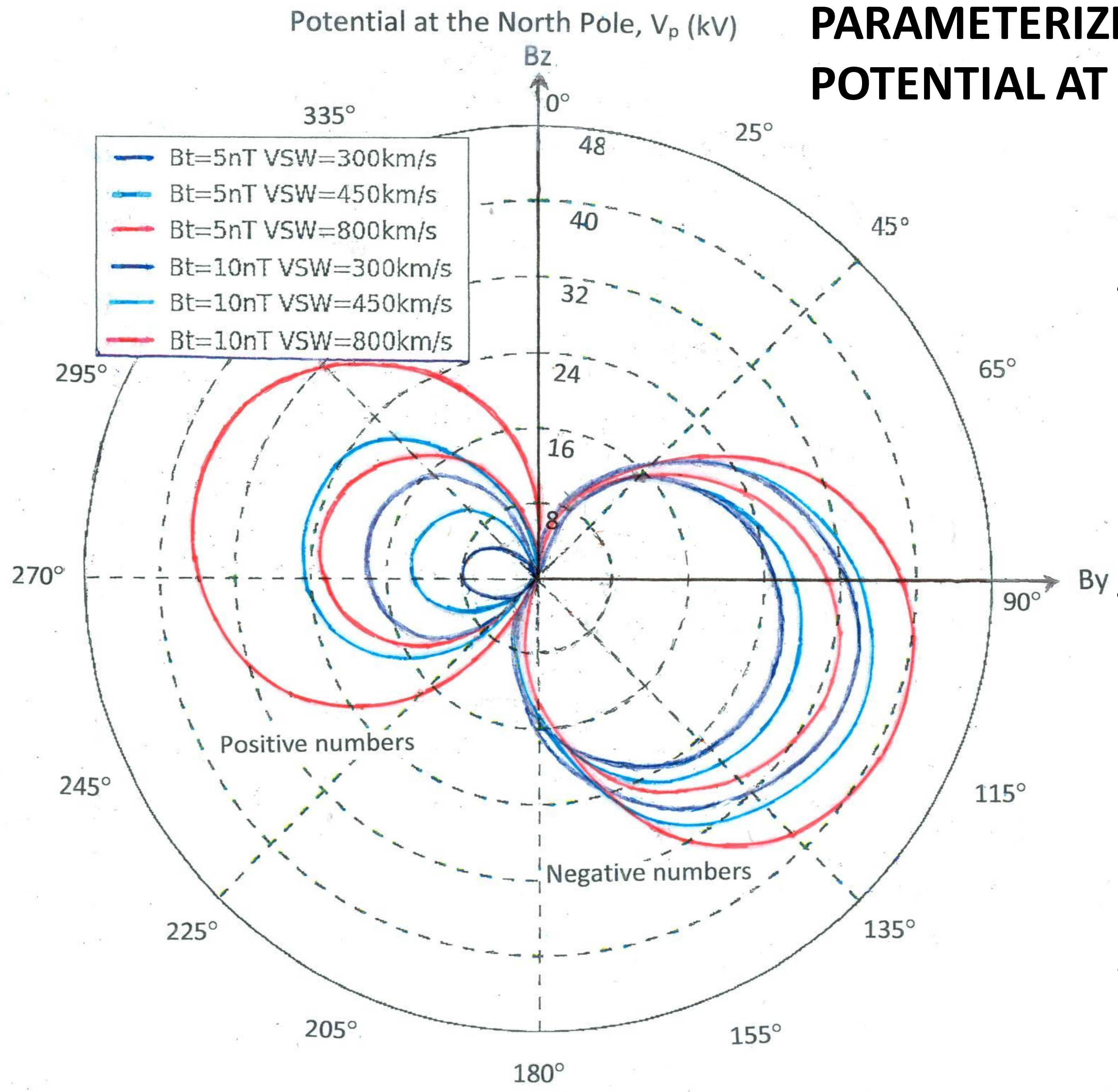

Using the Weimer (1996) satellite based empirical model:

Transverse IMF component, $B_T = \mathrm{Sqrt}(B_X^2+B_Y^2)$ has values 5 nT and 10 nT.

Solar wind speed is 300, 450 and 800 km/s.

The values of By and Bz determine the Clock Angle (0 to 360 degrees) in this plot.

We have parameterized the potential (VpN) as a function of transverse IMF, solar wind speed, and clock angle.

By, Bz, and SW Speed for July 2005 to June 2007 compared with same for July 2007 to June 2009

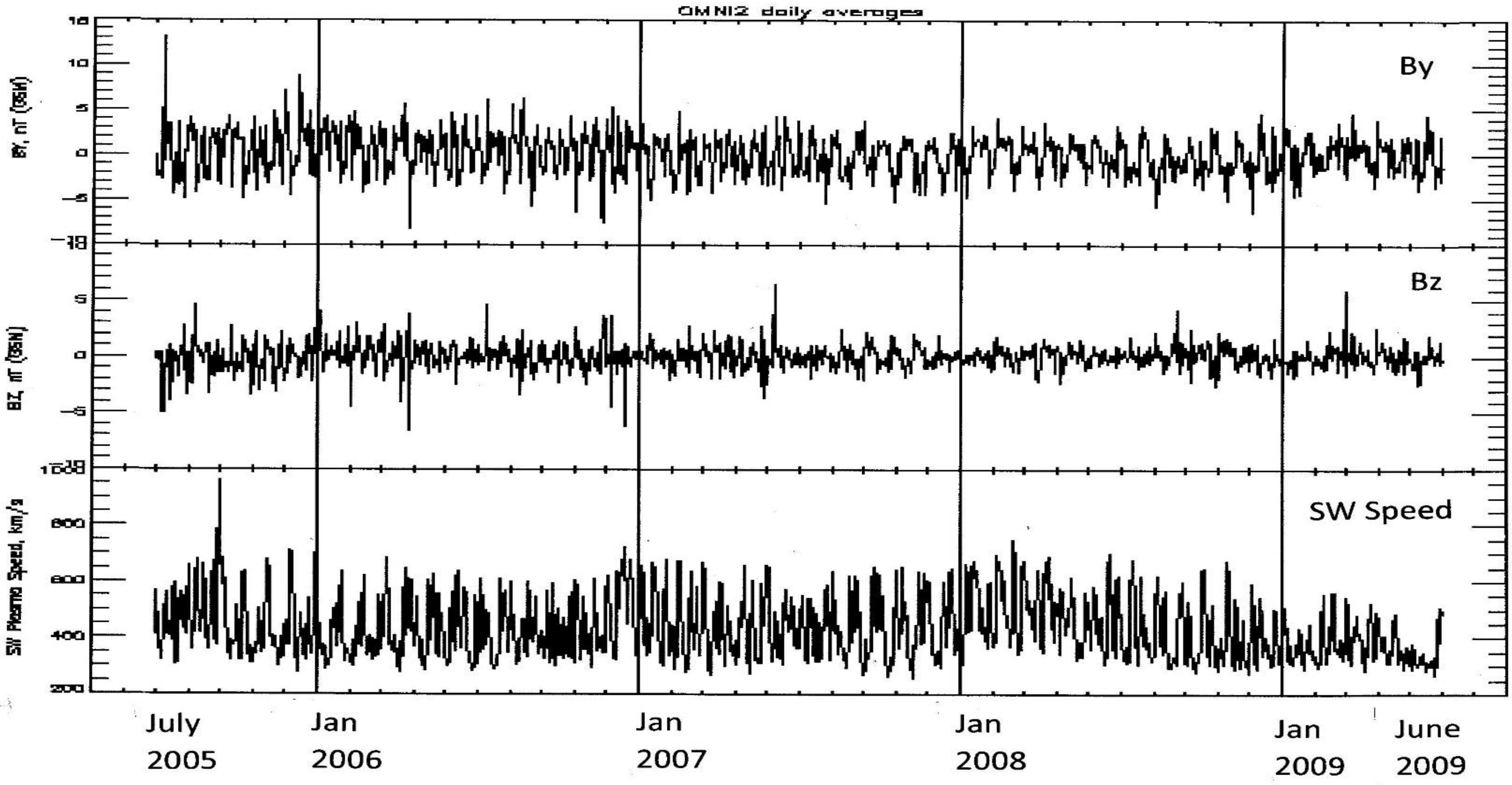

Correlation coefficients for downward longwave infrared responses at Alert to overhead ionospheric potential VpN, which is positive, as is Jz, when By is negative. Here we compare periods with predominantly 4-sector structure (blue) and 2-sector structure (orange). Note the predominance of the 27-day cycle with the 2-sector structure.

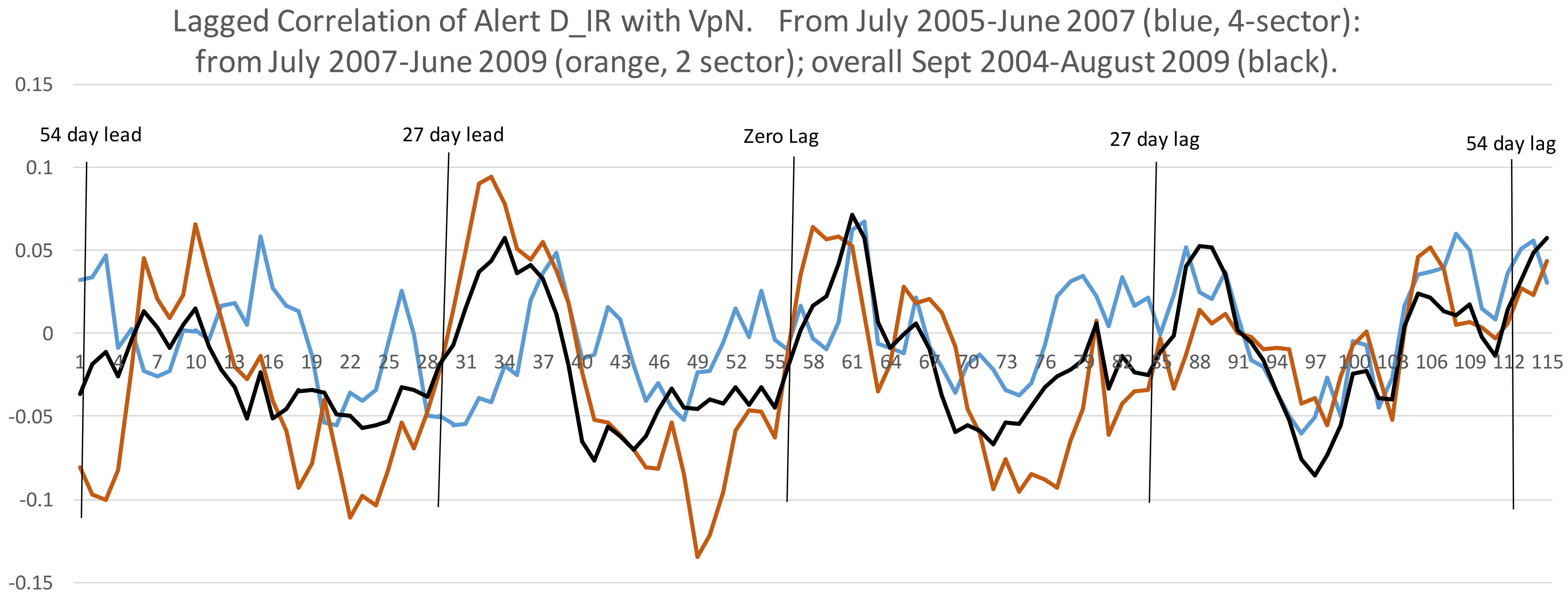

FOR PRESSURE ANALYSES: INTEGRALS OF SOLAR WIND IONOSPHERIC POTENTIAL OVER THE NORTHERN POLAR CAP

Dusk lobe, negative

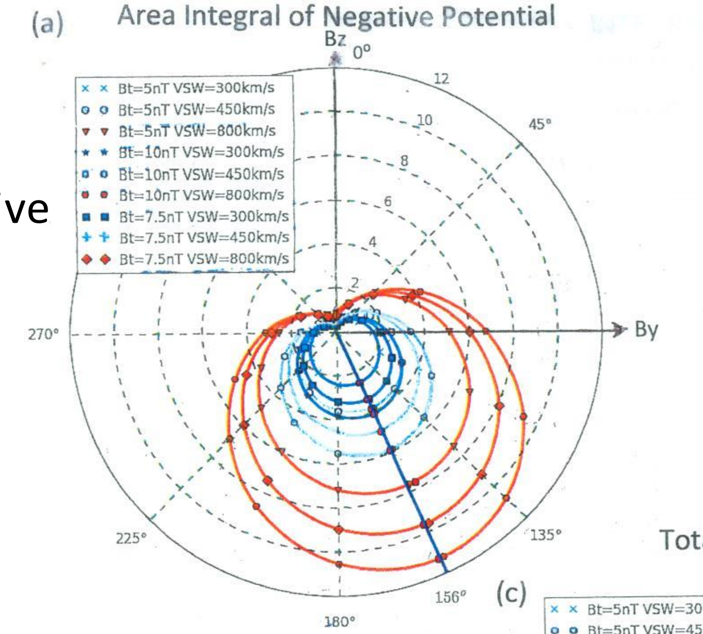

Dawn lobe, positive

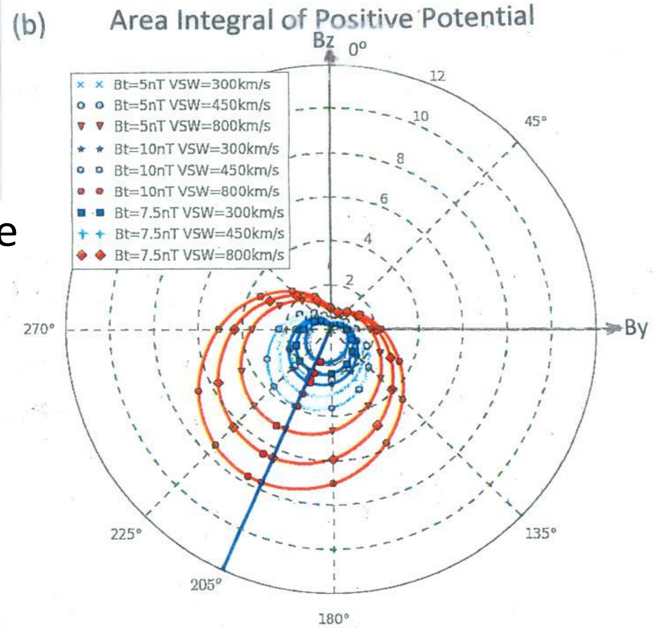

Plots show area-integrals of the negative (dusk) section and positive (dawn) section of the ionospheric potential distribution over the northern polar cap.

Units are 10^8 kVkm^2.

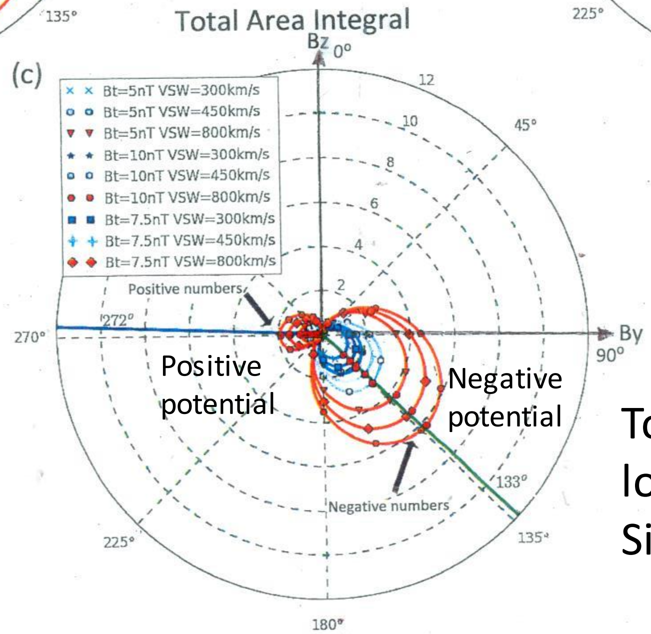

As with the plots of the potential at the pole, B_Y and B_Z determine the clock angle and B_T, the transverse IMF component. Solar wind speed is 300, 450, and 800 km/s. The negative potentials dominate the positive potentials in the total integral.

Total both lobes, SigmaN

As with the potential at the magnetic pole, we have parameterized the integrated potential as a function of Transverse IMF, Solar Wind Speed, and Clock Angle.

FLUCTUATIONS OF STANDARD DEVIATIOONS OF By AND VpN IN 27-DAY INTERVALS.

Maxima at solar max and in declining activity.

The effects of Bz enhance those of By and SW speed in the second half of the year in the N.H., when By and Bz have opposite signs, and partially cancel in the first half, when they have the same sign.

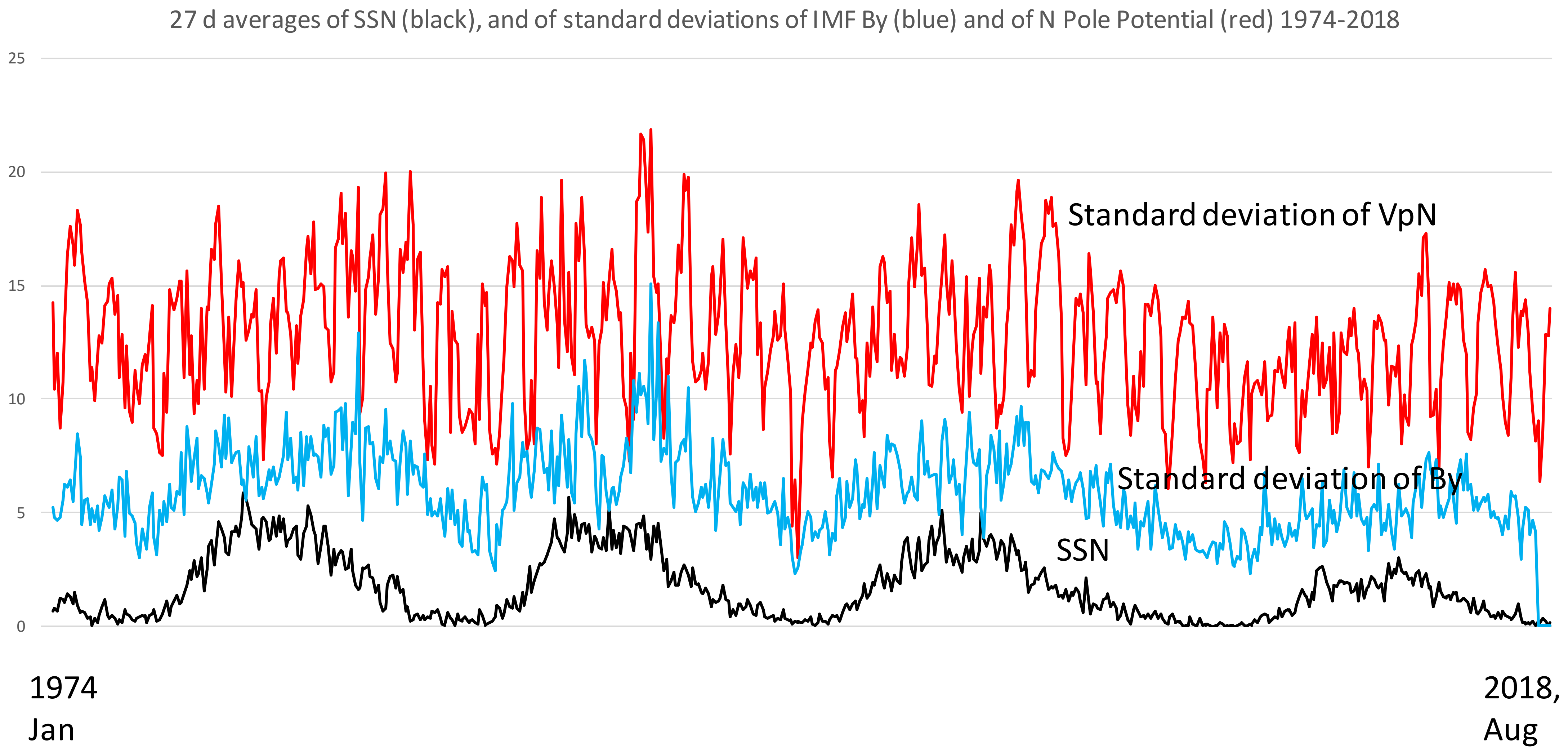

Hypothesized Mechanism: Growth of Ultrafine Aerosol Particles in Space Charge

Ultrafine (3-10 nm) aerosol particles predominate in Antarctic upper troposphere (Humphries et al., 2016). Varying with stratospheric sulfate, especially after volcanic eruptions.

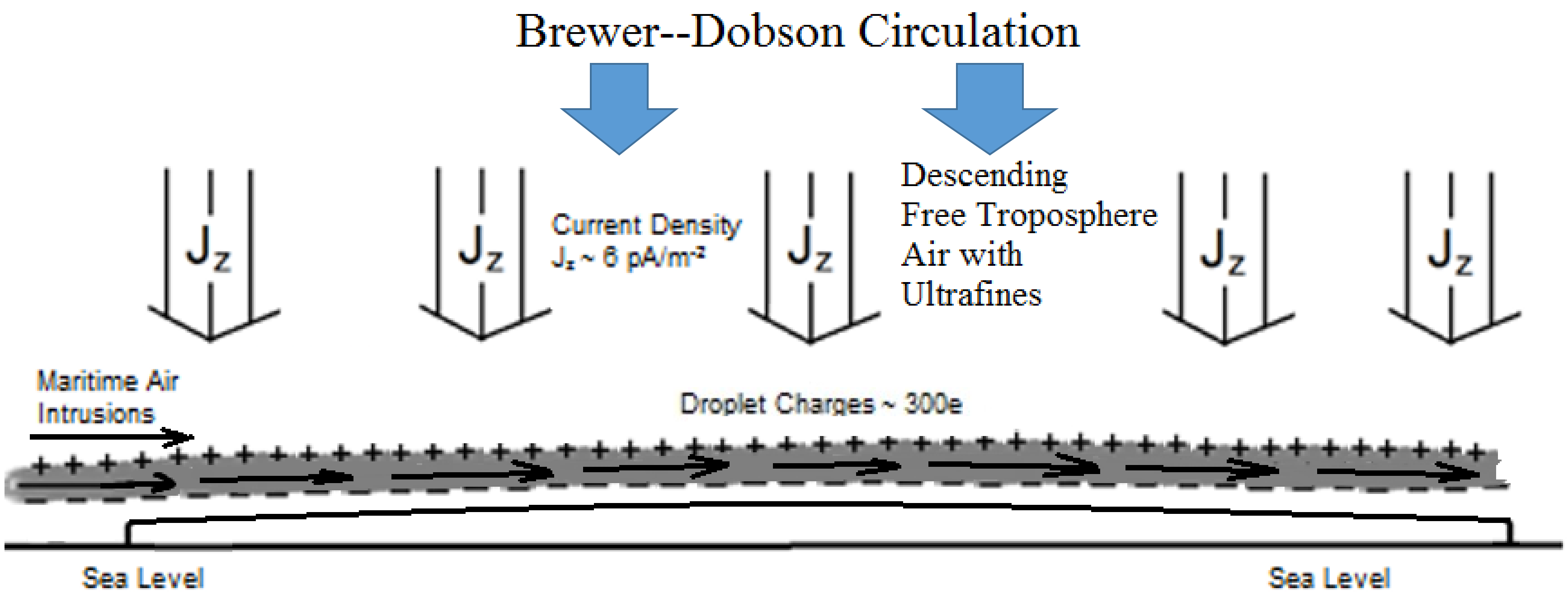

Electro-anti-scavenging in space charge layer inhibits coagulation of ultrafines: they can grow to CCN size in slowly changing stratus-type clouds. The air descending from the upper troposphere is enriched in ultrafine aerosol particles.

Increased CCN concentration increases cloud opacity by the Twomey effect.

Air and land surface warm and affect surface pressure and atmospheric dynamics.

See Zhou et al., JASTP, 2018; Zhang et al., JGR, 2018.

THE SOLAR WIND SECTOR BOUNDARY CONNECTION (SOLAR WIND SPEED, RELATIVISTIC ELECTRON FLUX, REDUCED MAGNETIC ACTIVITY, VOLCANIC AEROSOL).

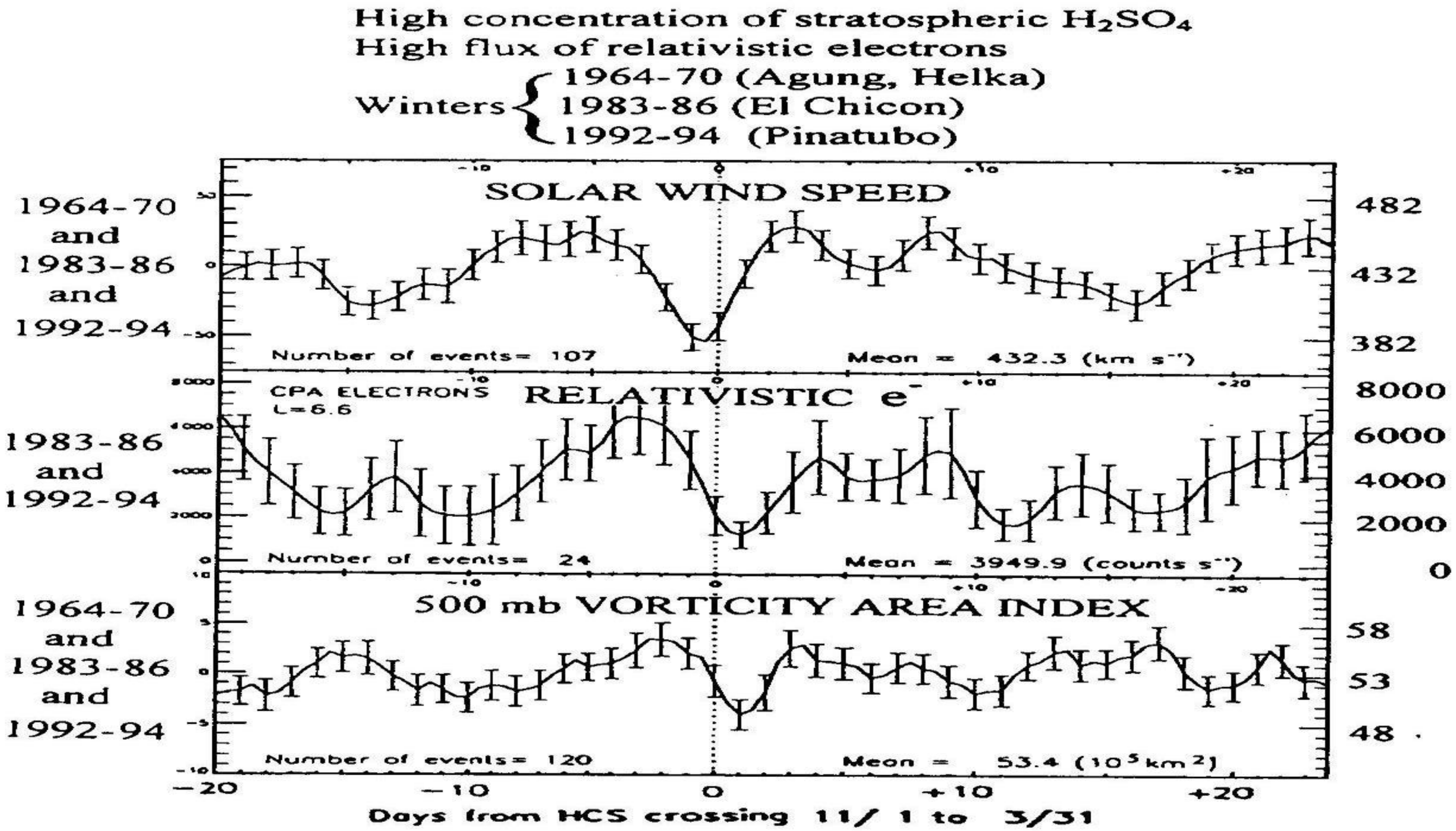

Superposed epochs, keyed to days of sector boundary crossings, November-March. Top: Solar wind speed.
Middle: MeV electrons from geosynchronous orbit.
Bottom: Northern hemisphere Vorticity Area Index.

Kirkland et al.,, 1996.

VORTICITY AREA INDEX, SOLAR WIND SPEED, AND RELATIVISTIC ELECTRON FLUX RELATIONS

From Mironova et al., 2011

The VAI response was only present in 1997-2002 at Vsw minima when the >2 Mev REP flux was <10^4 $cm^2 str^{-1} s^{-1}$

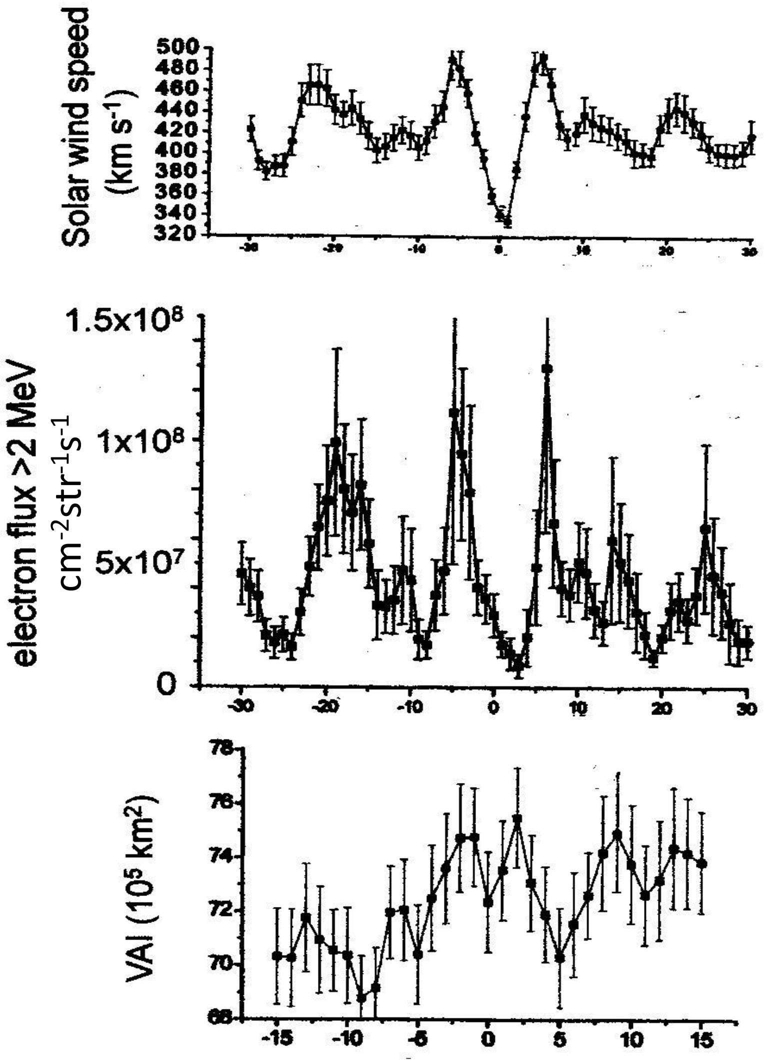

Key day: Minima in solar wind speed

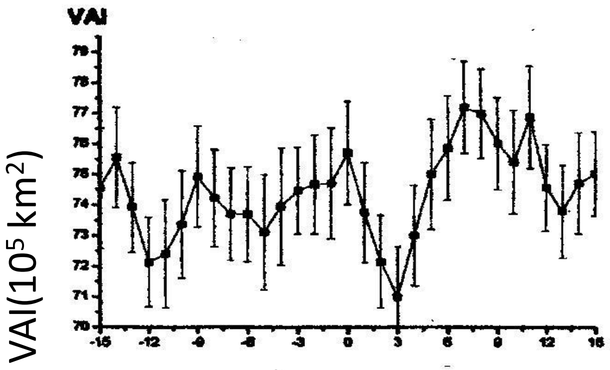

Key day: Minima in relativistic electron flux

RESPONSES OF THE NAO AND AO DAILY INDICES AT SOLAR WIND SPEED MINIMA.

The responses are only found with high concentrations of volcanic H_2SO_4 aerosol in the stratosphere.

147 SWS minima, 1963-2011.

From Zhou et al. Advances in Space Research, 2014

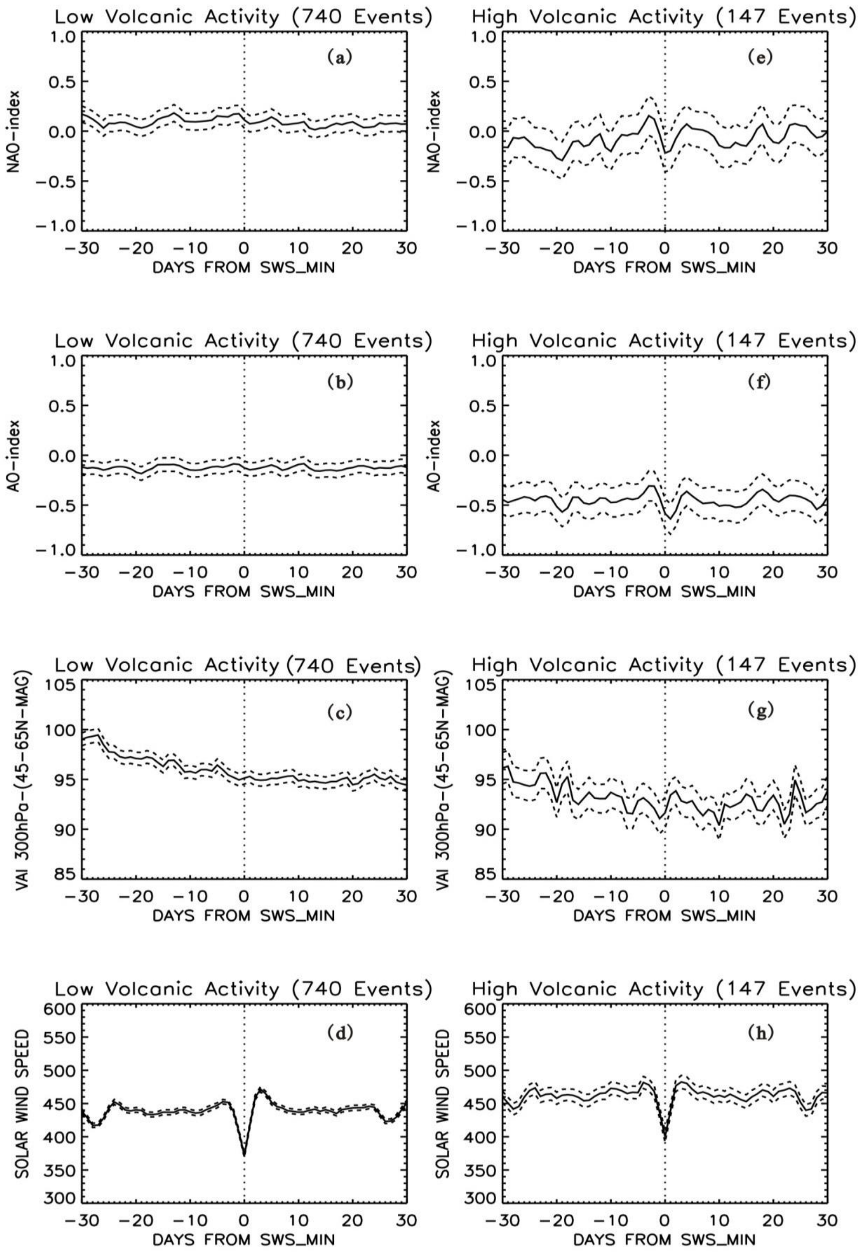

North Atlantic Oscillation Index

Arctic Oscillation Index

300 hPa Vorticity Area Index

Solar Wind Speed

COMPARISON OF NAO, SUNSPOT NUMBER, THEIR CORRELATION COEFFICIENT, AND STRATOSPHERIC AEROSOL LOADING

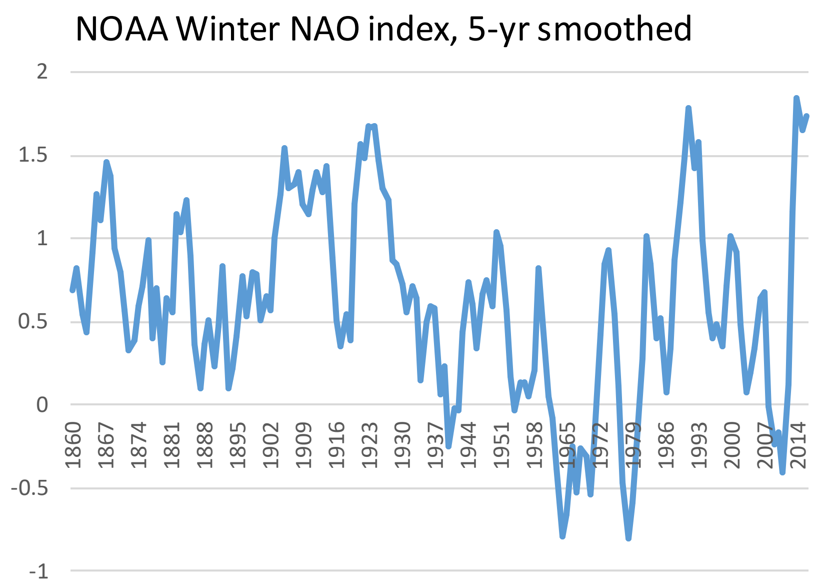

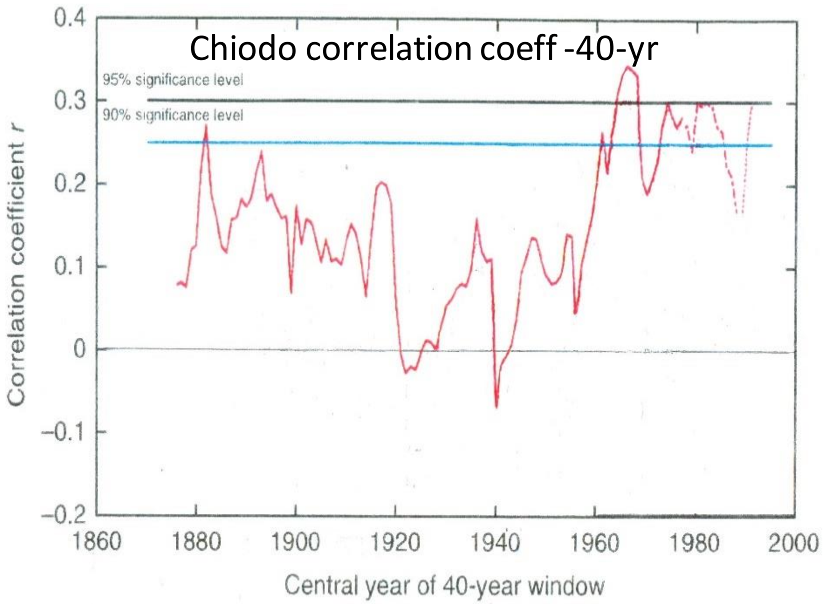

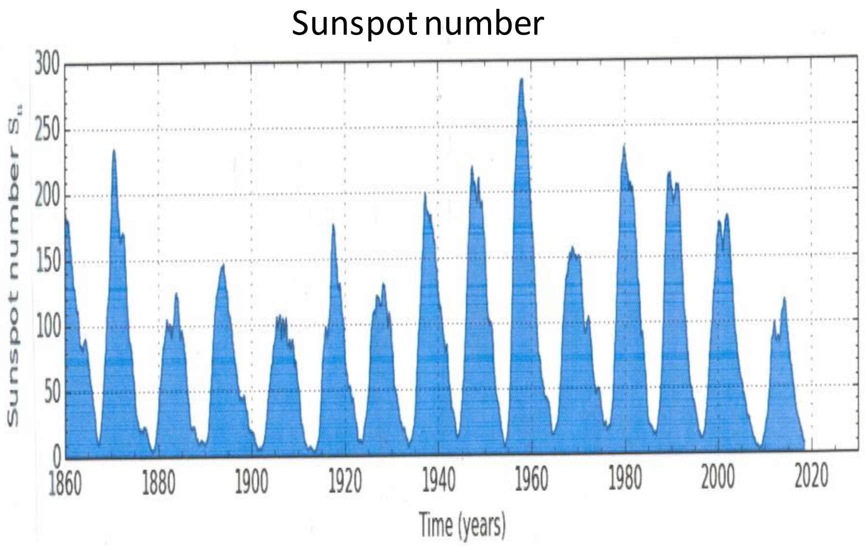

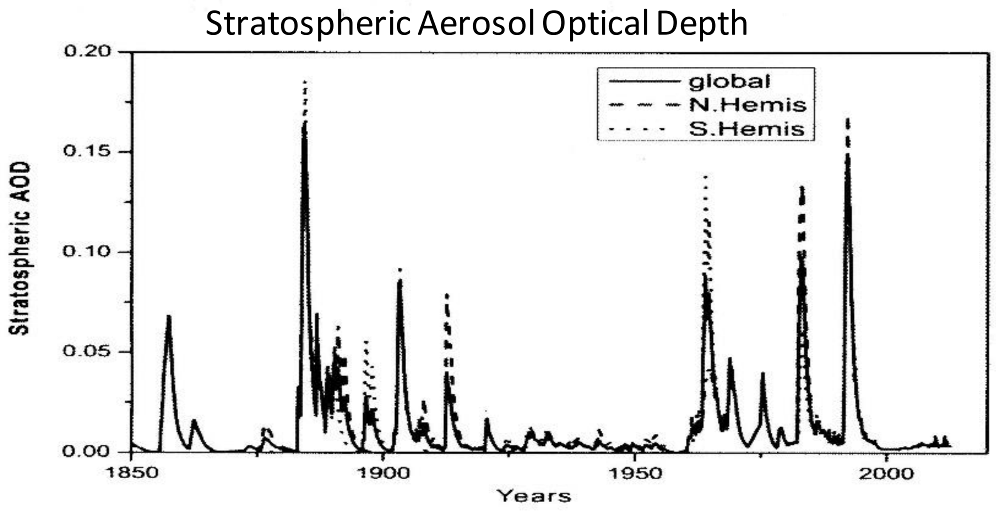

THE COSMIC RAY CONNECTION AND ITS LATITUDE VARIATION

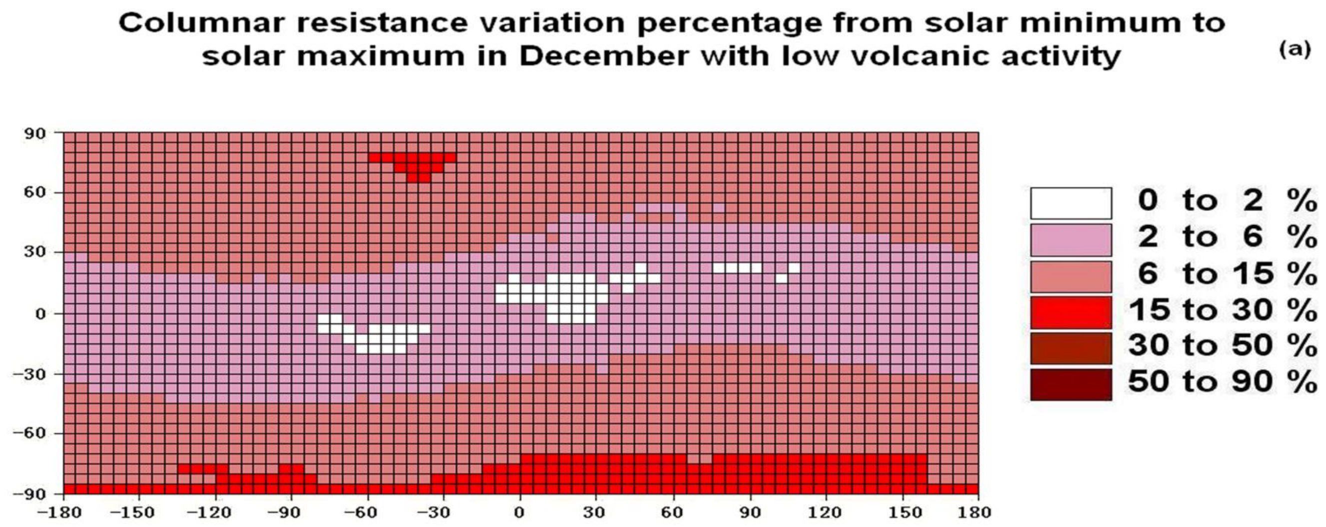

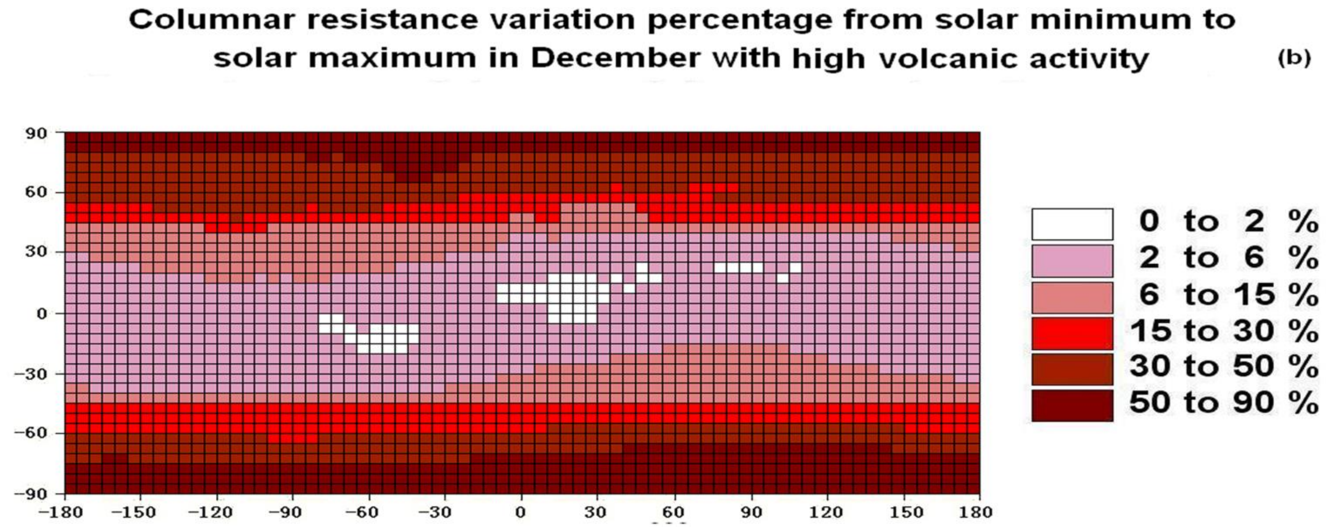

GLOBAL CIRCUIT COLUMN RESISTANCE VARIATION WITH SOLAR CYCLE (AND FORBUSH DECREASE) OF COSMIC RAY FLUX (Tinsley & Zhou, 2006)

DECADAL CLOUD COVER OVER THE USA

From Udelhofen and Cess, Geophys. Res. Lett., 28, 2617-2620, 2001

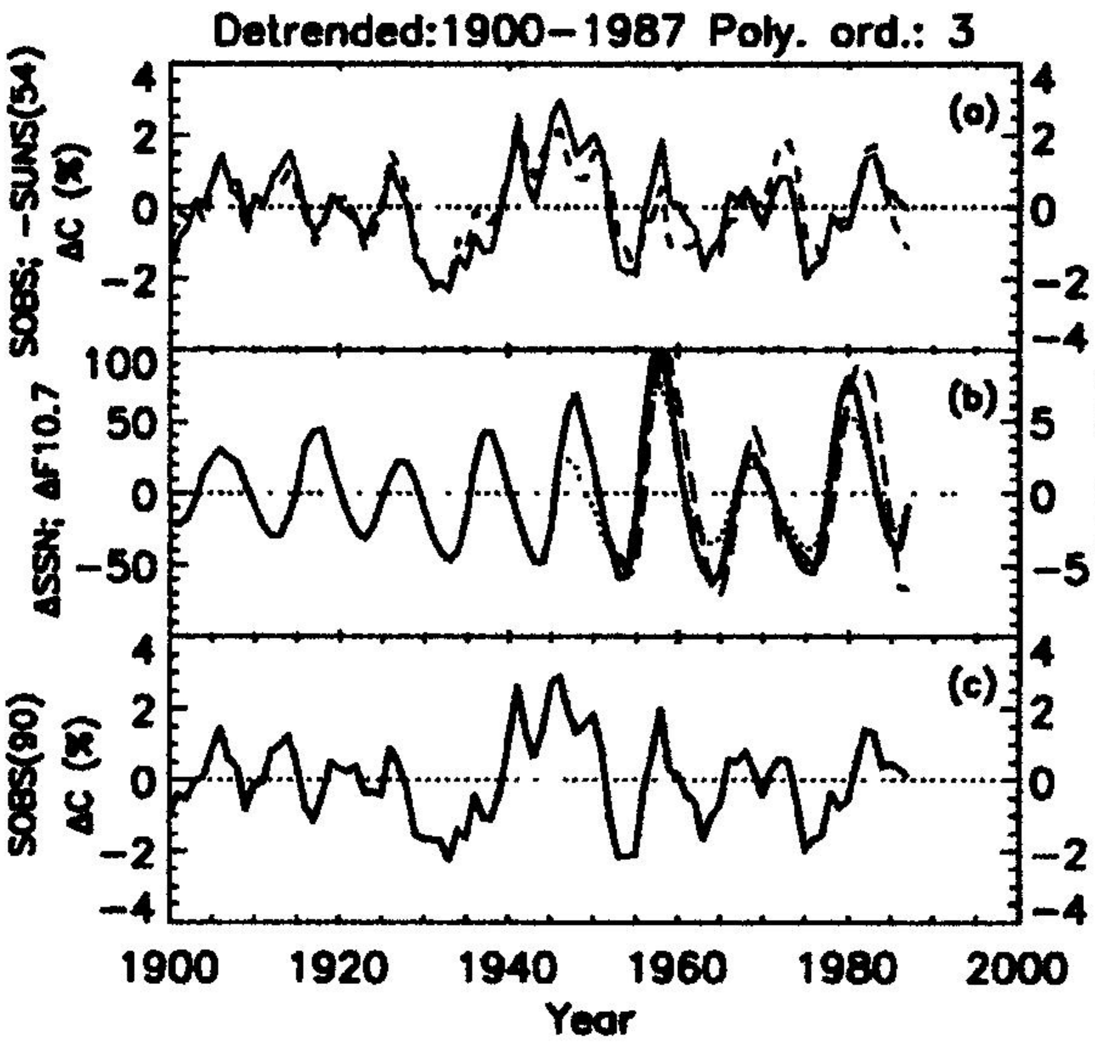

(a) Cloud cover anomalies (SOBS- solid line) and sunshine anomalies (dashed) (deviations from average) from 54 stations over the continental United States, 1900-1987.
(b) The 11-year solar cycle, as sunspot number (solid) and F10.7 (dotted), and as inverted cosmic ray flux (dashed).
(c) Cloud cover from 90 stations. Data smoothed with 3-year running mean. These cloud –solar cycle correlations are significant at the 95% level.

CLOUD COVER CHANGES IN NORTHERN ASIA

Pudovkin and Veretenenko, J. Atmos. Solar.-Terr. Phys, 57,1349-1355, 1995.

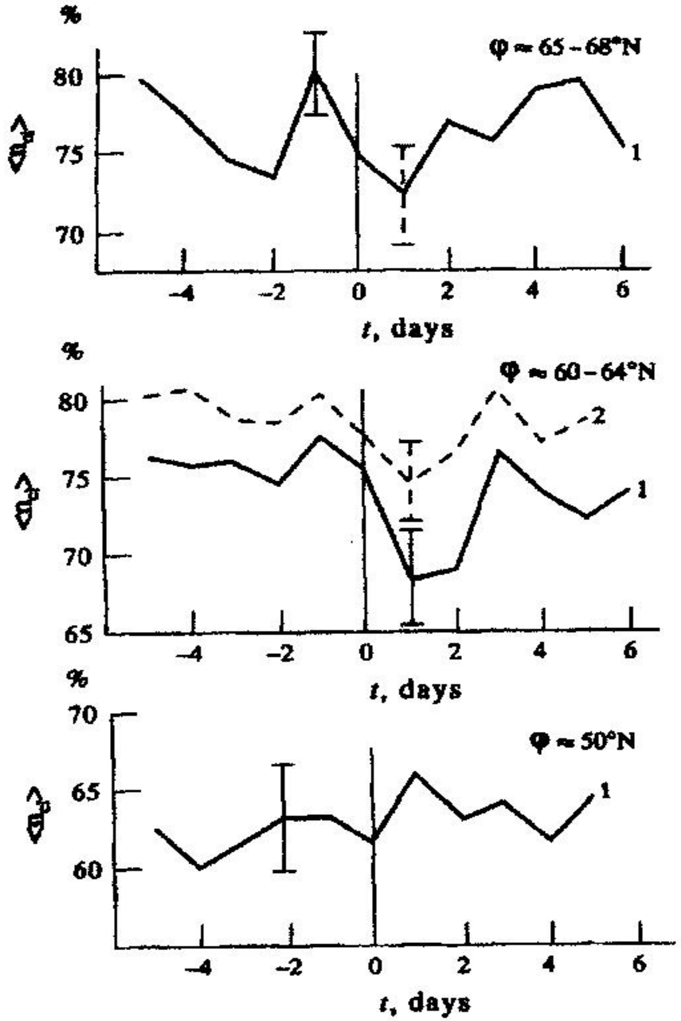

The fraction of total cloud cover in three different latitudinal belts 65-68N, 60-64N, and ~50N, for Actinic Observatories (ozone network) in the former Soviet Union, 1969-1986.
The key day (day 0) in the superposed epoch analysis was the day of onset of the Forbush decrease. The solid curves are for winter (42 events) and the dashed curve is for summer (21 events). The response on days 1 and 2 for 60-64N, is largest in winter, but is present at smaller amplitude in summer and for 65-68N.

DISCUSSION AND CONCLUSIONS

There appear to be a variety of ways in which day-to-day effects on clouds and atmospheric dynamics are produced by the solar wind:

In addition to thunderstorm effects on ionospheric potential there are :

(a) The IMF By input to ionospheric potential and Jz
(b) The magnetic activity (Ap) effect, which appears to be due to ionospheric potential and Jz changes
(c) The effects on atmospheric vorticity (mid-latitudes). These occur at sector boundaries when there are minina in relativistic electron precipitation and the presence of stratospheric volcanic aerosols.
(d) Effects of solar wind speed on the NAO in the presence of stratospheric volcanic aerosols.
(e) Effects of changes in atmospheric ionization due to cosmic ray Forbush decreases and the 11-year solar cycle (these and volcanic aerosols also change the latitude distribution of Jz).

We propose that the responses of clouds in (a) and (b) are due to increases in the concentration of droplets and /or ice particles in long-lived stratus – type clouds. The increase may be due to electro-anti-scavenging of ultrafine aerosol particles in the regions of excess charge of like sign just below the tops and just above the bases of the clouds. The electro-anti-scavenging allows the ultrafine particles to grow to CCN or IN size.

Other effects on clouds may be due to electro-scavenging inducing ice production and latent heat release

We propose that the variations in stratospheric aerosol concentration (c) has three effects:

(i) supplying part of the flux of ultrafine aerosol particles involved in electro-anti-scavenging responding to Jz

(ii) increasing the part of the column resistance at around 15 km altitude (this is where cosmic ray ionization maximizes, and so the solar cycle modulation of the column resistance and Jz then becomes more important).

(iii) for shorter periods increasing the column resistance to above 25 km. (this is where REP ionization maximizes, and so the solar wind modulation of REP and conductivity and Jz becomes more important).

THE SOLAR WIND POLAR CAP POTENTIAL CONNECTION; AN INPUT TO Jz

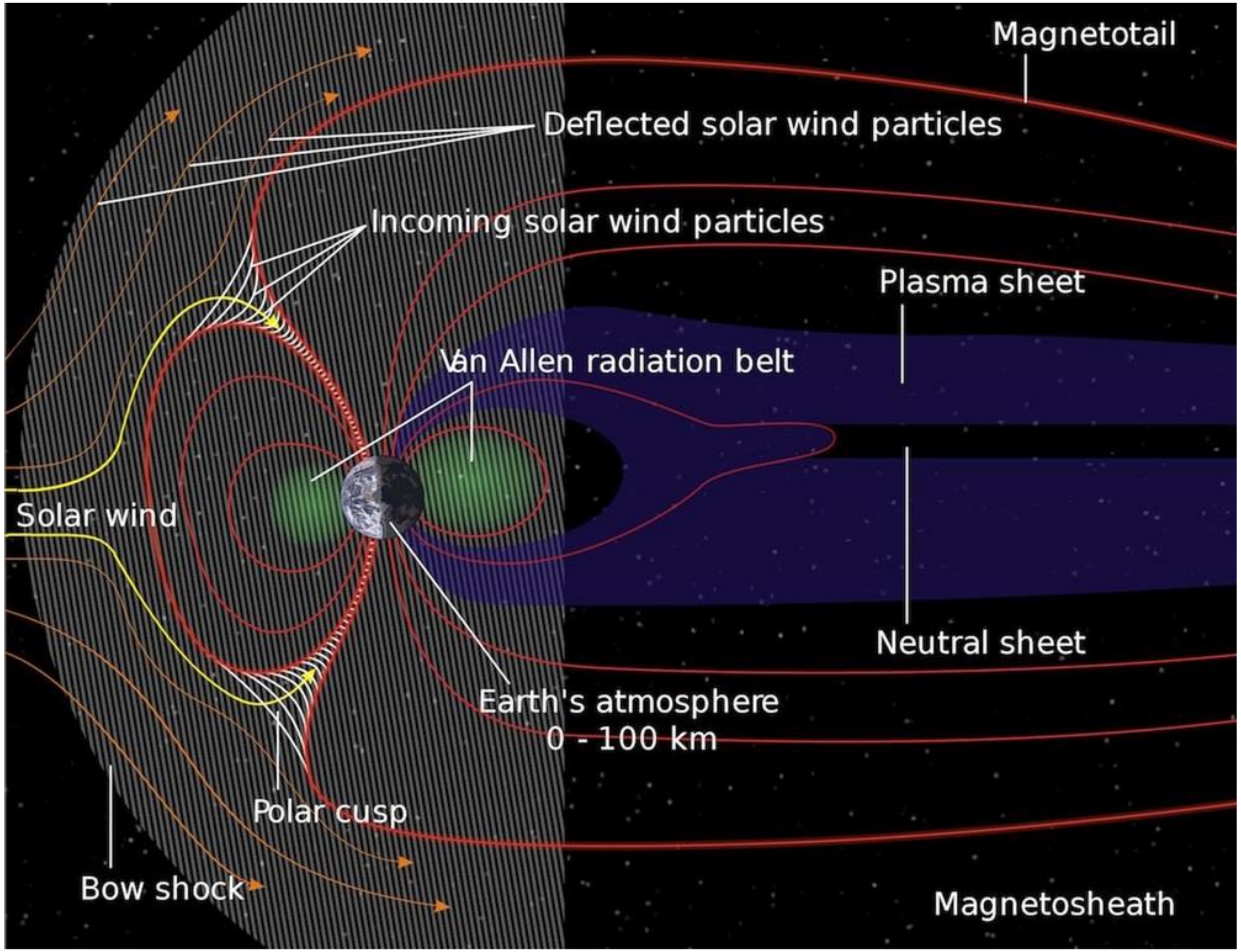

The relative speed between the magnetic fields in the solar wind is 300-800 km/s. The east-west (By) component of the solar wind ranges from -10 nT to +10 nT. The Earth's magnetic field lines running from cusp to cusp have high parallel conductivity. So the Lorentz electric field in the solar wind, $E = V_x x B_y$ generates a potential difference between the cusps, that is transmitted to the polar cap ionospheres.

POLAR CAP IONOSPHERE POTENTIALS from SOLAR WIND **V** x **B** FIELDS

(Markson, 1982)

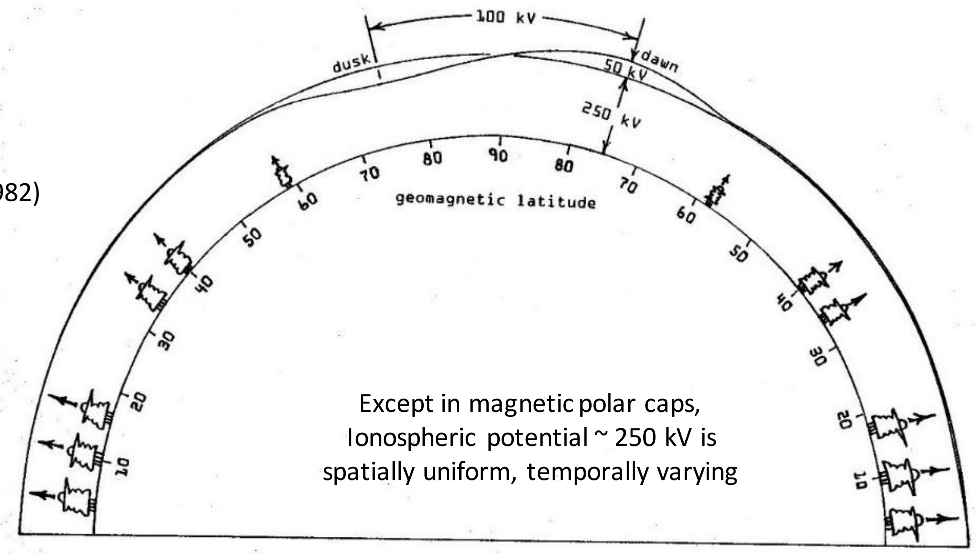

(Tinsley and Heelis, 1993)

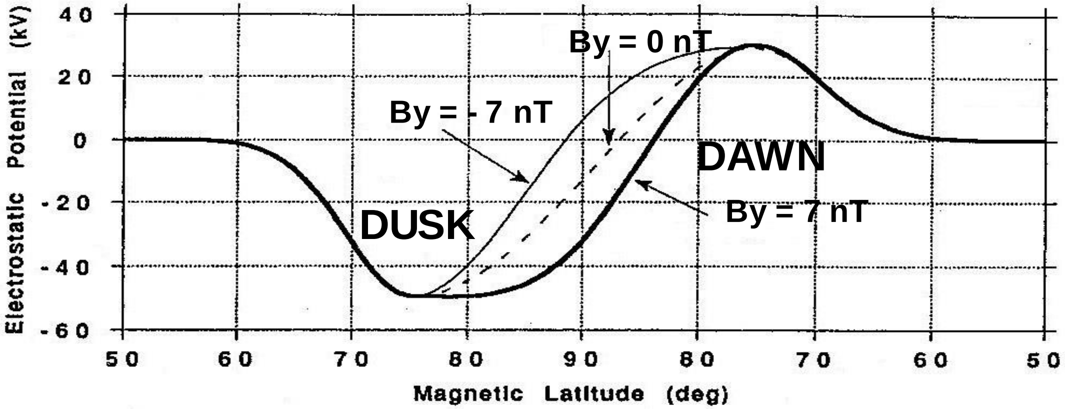

Within 30^0 of magnetic poles solar wind (**V**x**B**) electric fields generate potentials superimposed on the thunderstorm generated ionospheric potential.
The $\mathbf{B_z}$ component gives dawn and dusk potential excursions, maximizing 15^o from the magnetic poles and rotating with the sun.
The $\mathbf{B_y}$ component maximizes at the magnetic poles, due to the **V**x$\mathbf{B_y}$ electric field (north-south in space) raising the potential at the north M.P., while reducing it at the south M.P.

Lead-lag variations of the correlation coefficients (R-values) at the locations of strongest correlations in previous slide.

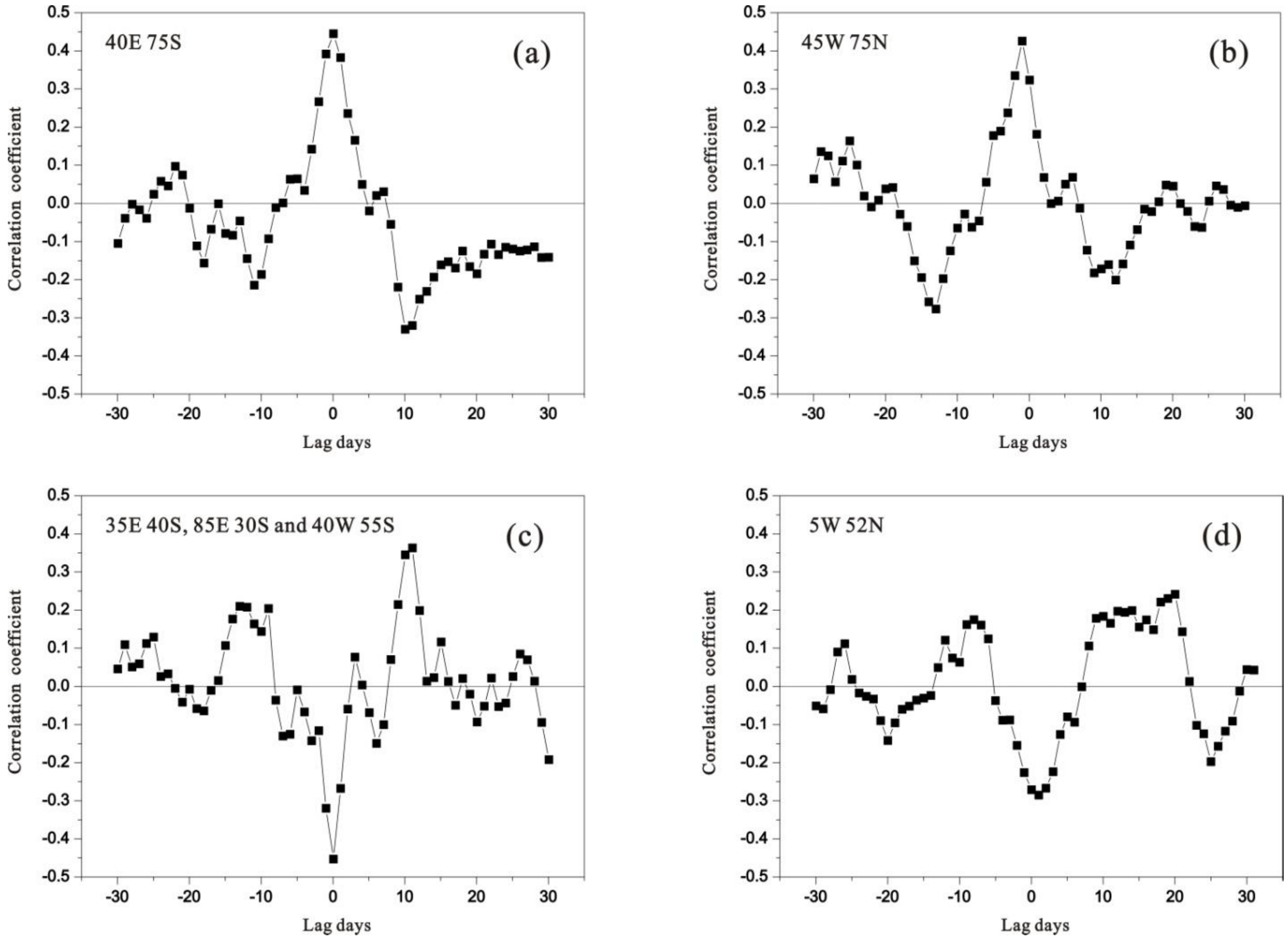

Zhou et al. 2018

The maxima or minima of surface pressures occur within 1 day of the Ez maximum

Symmetrical Atmospheric Charge gets concentrated into Asymmetric Space Charge at Tops and Bases of Layer Clouds by Ionosphere-Earth Current Density

Observations by Nicoll and Harrison, QJRMS, 2016

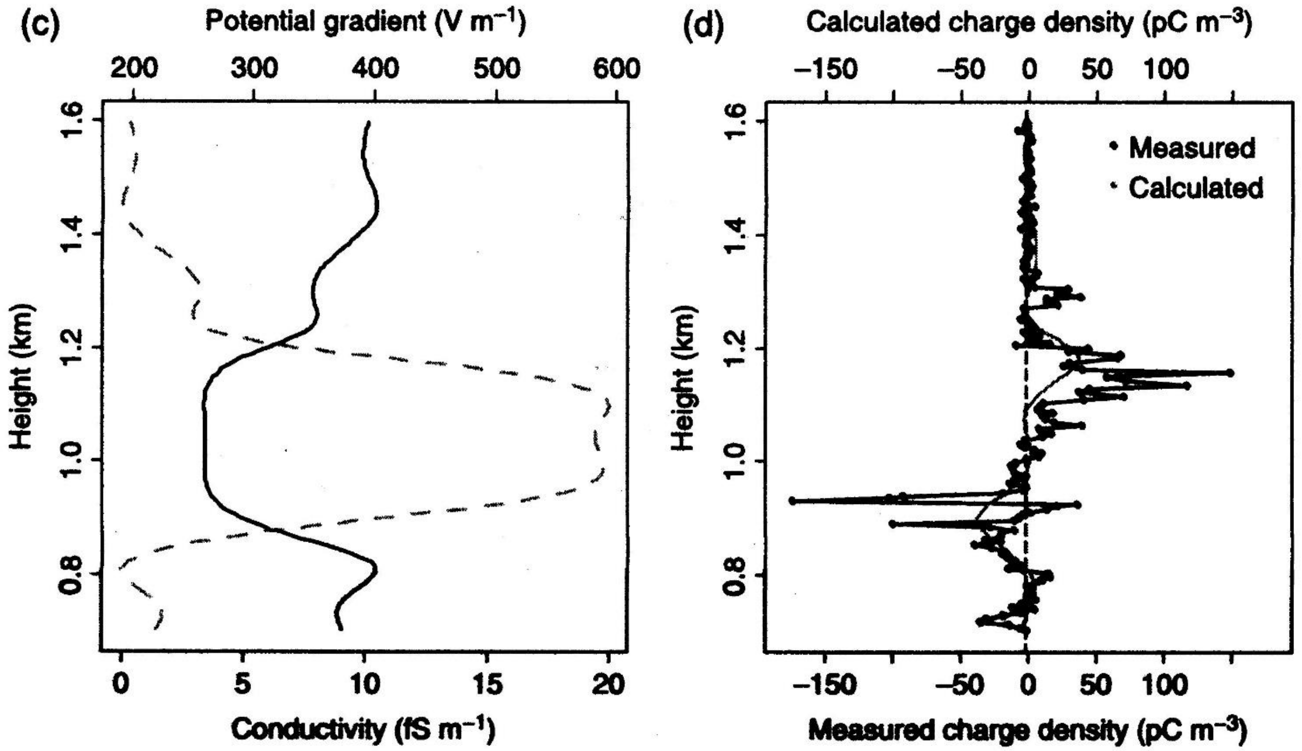

Reduction of conductivity (x3) is due to ion attachment in the cloud. Ionosphere-earth current density flows through cloud, generates potential gradients, which entail space charge at cloud top and base. Turbulence creates structure in the space charge.

Diffusion charging theory implies charges on aerosol particles and droplets proportional to the square root of their radii.

Aircraft and balloon data show clouds normally contain layers of such space charge (net unipolar charge).

THE SOLAR WIND SECTOR BOUNDARY (SOLAR WIND SPEED, RELATIVISTIC ELECTRON FLUX, REDUCED MAGNETIC ACTIVITY) CONNECTION TO Jz.

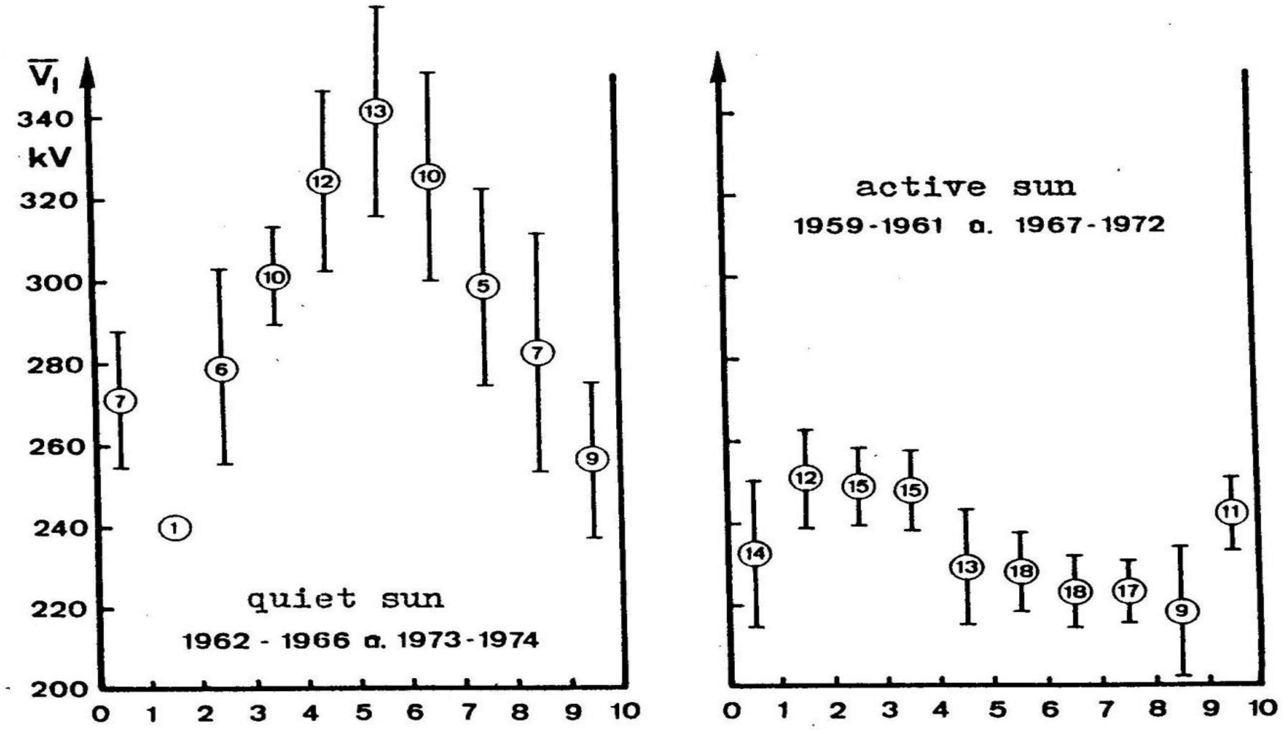

Potential from surface to 12 km from balloon soundings from southern Germany, sorted by position in solar wind magnetic sectors. Sector boundaries are at days 0 and 10. The period 1962-1966 corresponds to high concentrations of stratospheric sulfate aerosols (Agung) and the period 1959-1961 to very low concentrations of stratospheric aerosols.

H. J. Fischer and R. Mühleisen, "The ionospheric potential and the solar magnetic sector boundary crossings", Report Astronomisches Institut der Universität Tübingen, 1980.

OBSERVATIONS

Vorticity Area Index changes keyed to either HCS crossings or minima in relativistic electron flux minima, which produce minima in J_z

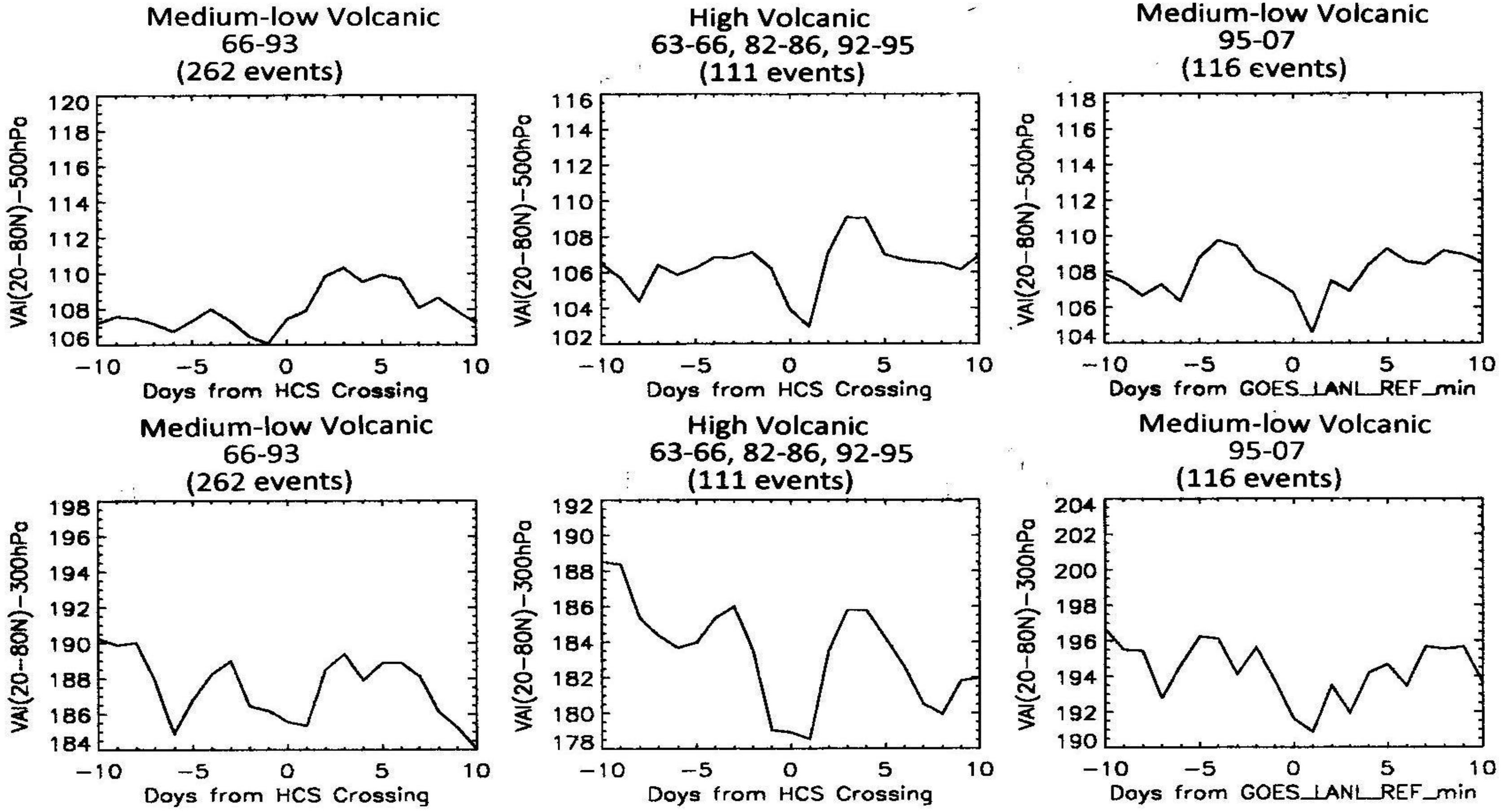

VAI response for medium-to-low stratospheric volcanic aerosol winters compared with high aerosol winters. Key days prior to 1995 are HCS crossings; from 1996 to 2007 are relativistic electron flux minima. From Tinsley et al. Adv. Space Res. 2012.

CLOUD COVER CHANGES WITH COSMIC RAY FORBUSH DECREASES OVER ANTARCTICA

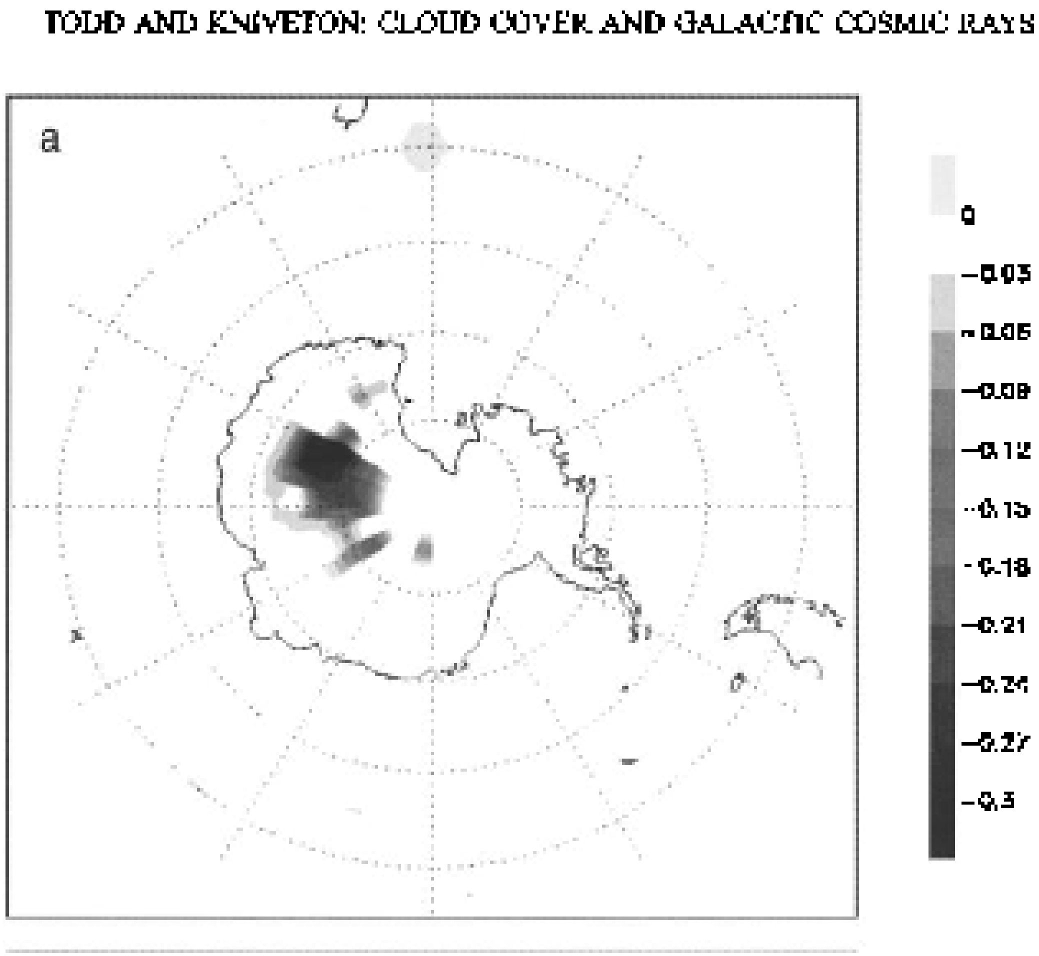

Todd and Kniveton, J. Geophys. Res., 2001.

Mean high cloud (10-180 hPa) anomalies on day 1 relative to reference level (day -5 to day -3) where day 0 is the day of onset of Forbush Decreases of galactic cosmic rays. 23 events. Only anomalies significant at the 0.05 probability level are shown. Maximum reduction of cloud cover ~ 30%.

Venne & Dartt: solar cycle NH wind speed and direction changes

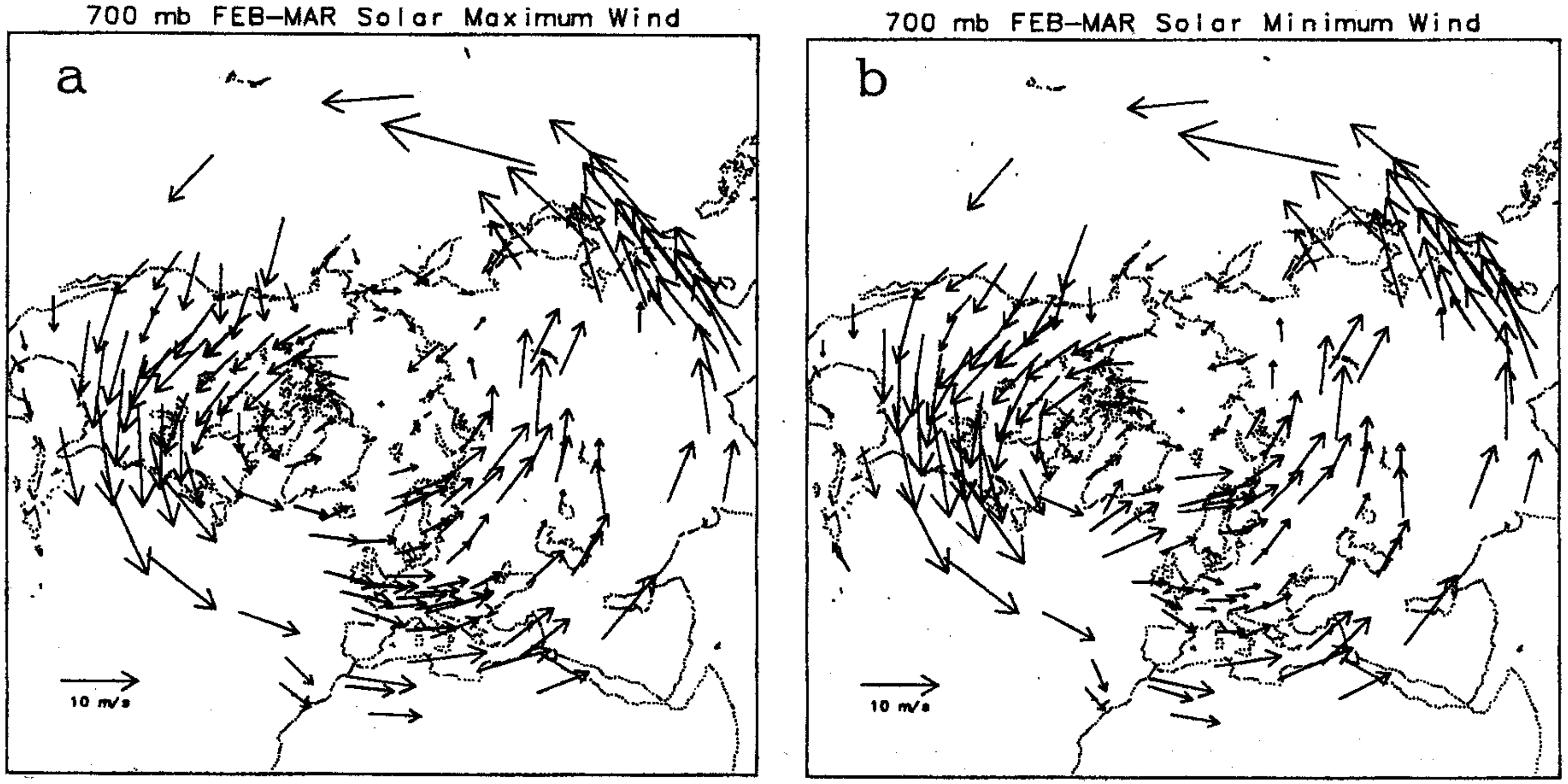

Winds at 700 mb in Feb.-Mar. for west QBO years 1950-1988 for (a) solar maximum years and (b) solar minimum years. From Venne and Dartt, J. Clim., **3**, 272-281, 1990.

SOLAR MODULATION OF THE BLOCKING IMPACTS ON THE NEAR-SURFACE (2-m) TEMPERATURE DISTRIBUTION 1955-1999

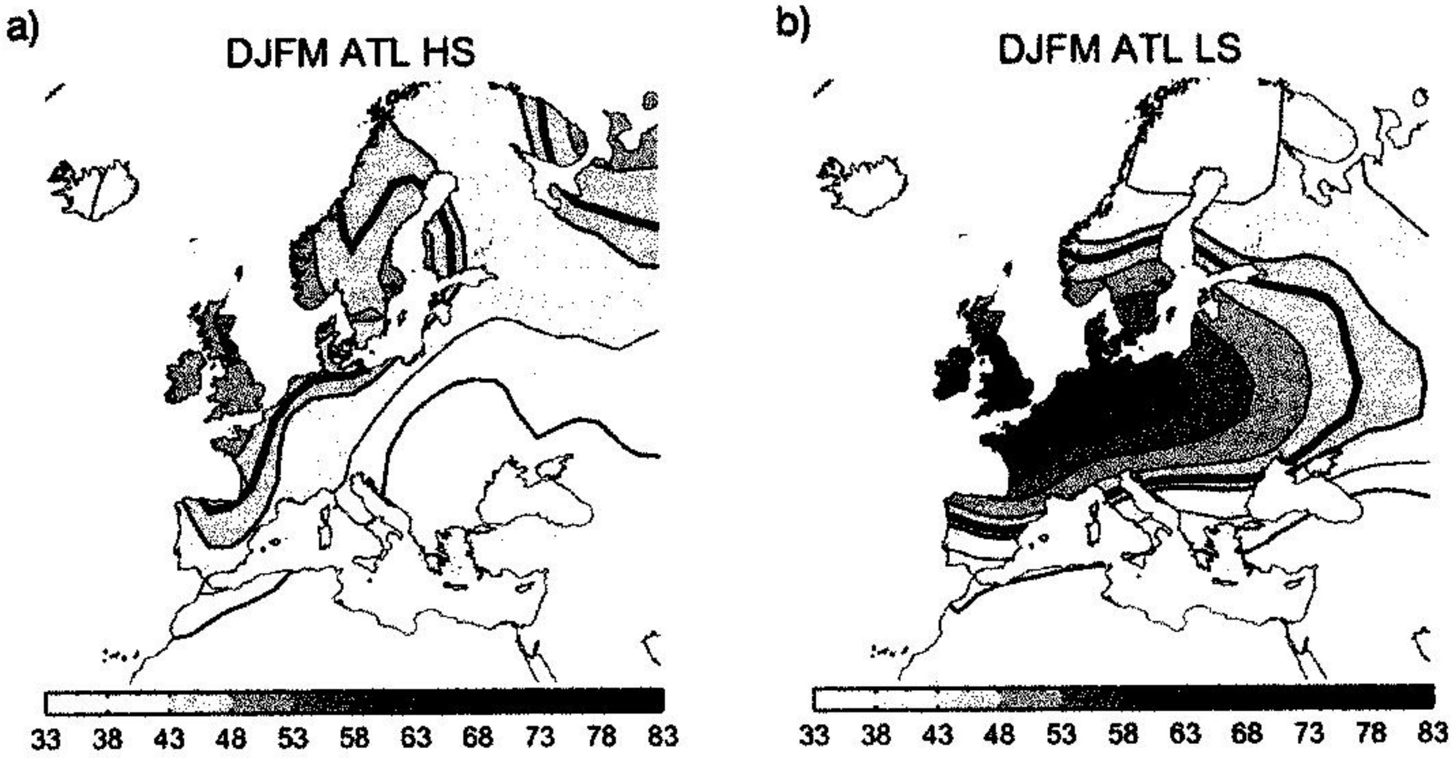

The climatological (all days) distribution of temperatures for all locations is first computed, and then the percentage of Atlantic blocking days with temperature anomalies in the lower tercile is computed with the blocking days sorted by (a) highest solar activity, and (b) lowest solar activity. The effects of LS blocking gives colder temperatures for most of Europe in which more than 50% of the blocking days are associated with temperature anomalies in the lower tercile. For HS the percentage of blocking only exceeds the expected value (33%) in northern Europe. Shaded areas denote those values exceeding 33%, with a 5% contour interval, and the solid line denotes the threshold for the confidence level of 95%. From Barriopedro et al., J. Geophys. Res., 113, D14118, 2008.